
THE UNIVERSITY of ADELAIDE

# Effect of Cement Contents on the Behaviour of Boreholes Drilled in Poorly Cemented Sandy Formations

By

Jun Hyuk Heo

Thesis submitted for the degree of

Doctor of Philosophy

The University of Adelaide

School of Civil, Environmental and Mining Engineering

Faculty of Engineering, Computer and Mathematical Sciences

November 2022

# Abstract

Drilling a borehole below the surface of the Earth is a mechanical process widely implemented by resource industries for various purposes, including geotechnical investigation and mineral exploration. Significant numbers of exploration boreholes are often drilled through poorly cemented formations worldwide, particularly in Australia, and often they result in technical difficulties such as stuck pipes. As such, the ability to predict the failure behaviour of poorly cemented formations due to borehole drilling is important for minimising borehole instability problems and designing effective borehole supports.

This thesis presents a series of journal and conference papers studying the effect of cement content on the failure behaviour of poorly cemented sandstones in the vicinity of borehole excavation by experimental and numerical methods. Three different cement contents have been considered.

There has been limited experimental research conducted to investigate the failure behaviour of poorly cemented sandstone using a convergence measuring device. In this research, a series of comprehensive laboratory studies were conducted to investigate the borehole deformation in poorly cemented sandstone rocks under different stress path regimes by using convergence measuring device (CMD) designed for laboratory scale studies. Synthetic thick-walled hollow cylinder (TWHC) specimens comprising of sand grains, Portland cement and water were prepared for this study.

Mechanical properties of the synthetic sandstone specimens were investigated by conducting UCS and triaxial compression (Hoek cell) tests. The CMD was deployed inside the TWHC specimen to measure the borehole deformation. Five different stress paths were applied to the specimens to investigate the effect of stress paths and three different cement agent contents (10%, 12% and 14%) were considered to study the effect of cement content on the borehole

failure. These laboratory studies showed that the stress path has a significant influence on the failure behaviour of the borehole.

Due to poor cementation and granular behaviour of poorly cemented formations, Discrete Element Method (DEM) was identified as the most appropriate numerical method for generating realistic numerical models. Numerical simulations were conducted to study the influence of micro-parameters of DEM model on the results obtained from laboratory studies poorly cemented sandstone specimens.

# Declaration

I, Jun Hyuk Heo, certify that this work contains no material which has been accepted for the award of any other degree or diploma in my name, in any university or other tertiary institution and, to the best of my knowledge and belief, contains no material previously published or written by another person, except where due reference has been made in the text. In addition, I certify that no part of this work will, in the future, be used in a submission in my name, for any other degree or diploma in any university or other tertiary institution without the prior approval of the University of Adelaide and where applicable, any partner institution responsible for the award of this degree.

I acknowledge that copyright of published works contained within this thesis resides with the copyright holder(s) of those works.

I give permission for the digital version of my thesis to be made available on the web, via the University's digital research repository, the Library Search and also through web search engines, unless permission has been granted by the University to restrict access for a period of time.

I also acknowledge the support I have received for my research through the provision of an Australian Government Research Training Program Scholarship.

Signature: Date: 21 November 2022

# List of Publications

The following directory presents a list prepared journal and conference papers authored by the candidate.

**Journal papers in the main research included in this thesis**

1. **Heo, J.H**, Melkoumian, N. & Hashemi S.S. (2022). Laboratory Studies on the Application of Convergence Measuring Device for Monitoring Borehole Deformation. *Academic Journal of Engineering Studies*, 3(1) (Published).
2. **Heo, J.H**, Melkoumian, N. & Hashemi S.S. (2022). Evaluating the Effect of Different Stress Path Regimes on Borehole Deformation using Convergence Measuring Device. *Geosciences* 12(9), 317 (Published).
3. **Heo, J.H**, Hashemi S.S. & Melkoumian, N. (2022). Study of Micro-parameters of DEM Model on the Laboratory Experiment Results Obtained from Poorly Cemented Sandstone. *Geosciences* (Published).

**Conference paper in the main research topic included in this thesis**

1. **Heo, J.H**, Melkoumian, N. & Hashemi S. S. (2018). Development and Application of Laboratory-Scale Convergence Measuring Device in Monitoring Borehole Condition. In *52$^{nd}$ U.S. Rock Mechanics/Geomechanics Symposium*. Seattle, the United States.

# Acknowledgements

I would like to thank my principal supervisor Dr. Noune Melkoumian and co-supervisor Dr. Sam S. Hashemi for their continued encouragement and support through the ups and downs of the journey towards preparation and submission of this thesis.

I would like to thank laboratory staff members, Mr. Simon Golding and Mr. Adam Ryntjes for their assistance with conducting the experiments.

Finally, I would like to extend my gratitude and appreciation to my parents and sister for their encouragement, support, and love.

I am grateful for the opportunity to conduct this research and acknowledge everyone who have assisted and contributed towards finalising this thesis.

# Table of Contents

# List of Figures

# Introduction

Drilling boreholes into the ground disturbs the local in situ stress field due to the stress concentration around the cavity. Under the stress concentration, weak bonding between the particles in poorly cemented sandy formation may break when there is inadequate cement agent present between the interfaces of sand grains. Borehole instability involving convergence can result in the borehole collapse in weak underground formations. Majority of oil and gas reservoirs are located in weak sedimentary formations where particles are not strongly bonded, resulting in weakening of the rock formation in the vicinity of the borehole and often leading to a borehole convergence (Bianco and Halleck, 2001). This causes the drilling operations to stop in extreme cases. Monitoring the borehole condition and gaining a better understanding on it is essential for early detection of instability issues and minimizing borehole failure.

This thesis focuses on investigating the borehole stability in poorly cemented sandstones. Poorly cemented sandstones are characterized by low strength, poor cementation and high porosity (Bosio and Kanji, 1998).

First chapter of the thesis presents laboratory studies on borehole deformation drilled through weak poorly cemented sandstone by using Convergence Measure Device (CMD). For this, a series of laboratory tests were conducted on thick-walled hollow cylinder (TWHC) specimens made of synthetic sandstone. Newly developed Convergence Measuring Device (CMD) has been deployed inside the TWHC specimens to accurately measure the changes in the borehole diameter in combination with the real-time visual monitoring of the borehole failure.

Second chapter presents laboratory studies on the effects of stress path regimes on the borehole behaviour in poorly cemented sandstone. For this, a series of laboratory based TWHC tests were designed and conducted. Both far-field and an element on the borehole wall were considered for applying different stress paths. The borehole deformation was monitored by the CMD. The borehole was also monitored by a video camera to record and determine the failure along the borehole walls for the specimens.

Third chapter presents studies using Discrete Element Method (DEM) on contributing parameters for the behaviour of poorly cemented sandy formations subjected to triaxial compression tests by developing DEM simulations of laboratory tests conducted. A comparison between experimental and numerical results was conducted to validate the outcome of the DEM simulations.

Fourth chapter presents development and application of a laboratory-scale convergence measuring device. The accuracy and performance of the CMD for the applications to monitor failure behaviour of poorly cemented formations near an opening and under different stress paths were studied.

Fifth and final chapter of the thesis presents concluding remarks and recommendations for further research on the area of failure behaviour analysis of poorly cemented sandy formations.

# Chapter 1

# Laboratory Studies on the Application of Convergence Measuring Device for Monitoring Borehole Deformation

# (Journal Paper 1, Published)

Jun Hyuk Heo, Noune Melkoumian and Sam S. Hashemi

School of Civil, Environmental and Mining Engineering

The University of Adelaide, SA 5005, Australia

Publication:

Heo, J. H., Melkoumian, N. & Hashemi S.S. (2022). Laboratory Studies on the Application of Convergence Measuring Device for Monitoring Borehole Deformation. *Academic Journal of Engineering Studies, 3(1)*

# Statement of Authorship

| | |
|---|---|
| Title of Paper | Laboratory Studies on the Application of Convergence Measuring Device for Monitoring Borehole Deformation |
| Publication Status | ☑ Published ☐ Accepted for Publication<br>☐ Submitted for Publication ☐ Unpublished and Unsubmitted work written in manuscript style |
| Publication Details | Heo, J. H., Melkoumian, N. & Hashemi S.S. (2022). Laboratory Studies on the Application of Convergence Measuring Device for Monitoring Borehole Deformation. Academic Journal of Engineering Studies, 3(1) |

## Principal Author

| | |
|---|---|
| Name of Principal Author (Candidate) | Jun Hyuk Heo |
| Contribution to the Paper | Development of the Convergence Measuring Device, performed lab experiments, data analysis, manuscript development and publishing. |
| Overall percentage (%) | 70% |
| Certification: | This paper reports on original research I conducted during the period of my Higher Degree by Research candidature and is not subject to any obligations or contractual agreements with a third party that would constrain its inclusion in this thesis. I am the primary author of this paper. |
| Signature | Date 02/09/2022 |

## Co-Author Contributions

By signing the Statement of Authorship, each author certifies that:

i. the candidate's stated contribution to the publication is accurate (as detailed above);

ii. permission is granted for the candidate in include the publication in the thesis; and

iii. the sum of all co-author contributions is equal to 100% less the candidate's stated contribution.

| | |
|---|---|
| Name of Co-Author | Dr. Noune Melkoumian |
| Contribution to the Paper | Conceptualisation, supervision and review of the manuscript. |
| Signature | Date 25.09.2022 |

| | |
|---|---|
| Name of Co-Author | Dr. Sam S. Hashemi |
| Contribution to the Paper | Methodology, supervision and review of the manuscript. |
| Signature | Date 02/09/2022 |

Please cut and paste additional co-author panels here as required.

# Abstract

Borehole convergence or the change in borehole diameter during or after drilling is one of the primary indicators of borehole instability. Early recognition of borehole instability is critical in achieving successful and timely completion of drilling operations and for borehole exploitation. Commonly used borehole monitoring devices, such as caliper log and the acoustic borehole televiewer, provide limited attempts have been made to accurately measure the borehole diameter changes in laboratory scale studies. In this study, a series of laboratory experiments were conducted on Thick-Walled Hollow Cylinder (TWHC) specimens made of synthetic poorly cemented sandstone, where a new laboratory-scale Convergence Measuring Device (CMD) was deployed inside the borehole for monitoring the deformation of the borehole walls. This new CMD was developed based on the concept of Local Deformation Transducer (LDT). Three different cement contents (i.e., 10%, 12%, and 14%) and various lateral confining stress conditions (i.e., 2 MPa, 4 MPa and 6 MPa) were considered to evaluate the performance of the CMD. The specimens with CMD were tested using a modified Hoek cell which enabled visual monitoring of the borehole convergence and borehole wall breakout processes during the tests. The results showed that the CMD was capable of accurately measuring the borehole deformation. Visual monitoring of the borehole allowed precise identification of the locations and shapes of the borehole wall breakouts. Studies showed that the amount of the cement content and the magnitude of the lateral confining stress have a significant effect on the borehole deformation and failure stress. Furthermore, it was observed that the rate of increase in the radial strain of the TWHC specimens prior to the initiation of a borehole wall failure decreases when the cement content was increased.

Keywords: Borehole deformation; Borehole monitoring; Convergence measuring device; Thick-walled hollow cylinder; Laboratory study; Poorly cemented sandstone

# 1. Introduction

Drilling exploration boreholes into the ground is one of the most widely used methods for investigating the subsurface formations in energy and mineral resources industry. As with any other excavation, drilling a borehole disturbs local pre-existing stresses in the vicinity of the opening, and this may result in rock failure due to the induced local stresses exceeding the rock strength. In practice, borehole instabilities may occur seemingly unpredictably at any stage of the drilling operations, resulting in the loss of time and equipment, as well as, in extreme cases, in abandoning the borehole (Fjar et al., 2008). It has been estimated that about 70 % of the world's hydrocarbon reservoirs are found within poorly cemented formations, where borehole instabilities are most likely to occur (Bianco and Halleck, 2001). Furthermore, a significant number of exploration boreholes being drilled through poorly cemented formations worldwide, and particularly in Australia, often result in technical difficulties such as stuck pipes (Hashemi et al., 2015).

Borehole instability problems typically account for 5-10% of the total drilling costs and add up to the annual cost of hundreds of millions of dollars worldwide (Al-Ajmi and Zimmerman, 2006). Therefore, predicting the poorly cemented rock behaviour in the vicinity of excavation is essential for maintaining its stability and, consequently, for reducing the drilling costs. This study introduces a new laboratory-scale convergence measuring device (CMD) that has been developed for continuous real-time monitoring of the borehole deformation in TWHC specimens during the laboratory tests. Test results show, that the proposed CMD is an ideal tool for such applications. Unlike the commercially available CMDs such as the convergence meter, convergence monitor and borehole extensometer, which size and shape are designed for field applications primarily (Li, Feng & Hudson 2012), the proposed CMD is free from this limitation since it has been specifically designed for laboratory applications. In this work, laboratory studies on the stability of a borehole drilled through weak poorly cemented

sandstone were conducted through a series of TWHC tests, where, in combination with the real-time visual monitoring of the borehole failure, newly developed CMD has been applied to accurately measure the changes in the borehole diameter.

### *1.1. CMD Background*

Predicting and managing formation deformation in the vicinity of underground openings is an important aspect in the design and assessment of the performance of various geotechnical structures, such as tunnels, deep excavations, wellbores, and boreholes. Although some field studies can be conducted on this, most comprehensive studies are laboratory-based and use small-scale models, such as TWHC specimens for laboratory testing. The accurate measurement of the borehole convergence in these TWHC specimens has been one of the challenging topics of geomechanics in recent decades. Hight, Gens, and Symes (1983) developed a hollow cylinder apparatus for investigating the effects of principal stress rotation in soils. Tronvoll (1992) employed a clip gage for measuring the borehole convergence in TWHC tests. Rawlings et al. (1993) used a diameter caliper to measure the change in the borehole diameter of TWHC specimens by measuring it before and after the triaxial tests. O'Kelly and Naughton (2008) used proximity transducers that measure the radial displacements in the hollow cylindrical specimens. Papamichos et al. (2010) measured the borehole strain using an internal radial cantilever. Bujok et al. (2013) studied the convergence of the abandoned shallow oil wells through experimental modelling focused on the effects of borehole convergence on its deformation shape. Recently, Wu et al. (2016) used a borehole gage to measure the change in the borehole diameter during the borehole stability experiment. These studies focused primarily on the convergence measurement without the real-time visual monitoring of the borehole during testing. In this work, a new application of the local deformation transducer (LDT) has been considered and used for the development of the proposed CMD, with the aim of allowing accurate measurement of the borehole convergence

under various stress conditions. The basic principle of the suggested CMD is similar to that of the LDT which was originally proposed by Goto et al. (1991) to minimize the error present in the axial strain measurements from the triaxial testing. In designing and manufacturing the CMD, strain gages have been used. This is a common practice in designing transducers that convert a mechanical change, such as displacement, into a change in the voltage signal that is monitored after calibrating.

# 2. Experimental Study

*2.1 Laboratory facilities*

The uniaxial compressive strength (UCS), triaxial and TWHC tests are the most commonly used laboratory experiments for determining the parameters required for borehole stability analysis and understanding the behaviour of a granular formation under different stress conditions. In this study, the borehole stability experiments were performed on TWHC specimens in a modified Hoek Cell. The TWHC specimens had an external diameter of 63.5 mm, the internal diameter of 15 mm, and a height of 127 mm. During each test, the TWHC specimen was subjected to axial stress along the borehole axis, and the confining stress was provided by a servo-controlled hydraulic device. A number of laboratory facilities were used for conducting the tests. For applying vertical stress to the specimen, a servo controlled axial loading system of 300 kN capacity with 0.1 N accuracy was used. For applying and maintaining the external confining pressure at a very low level, the Hoek cell connected to an automatic hydraulic machine, which had a relief valve and a pressure gage with an accuracy of 0.01 MPa, was used. CMDs were placed inside the borehole of the TWHC specimen for measuring the borehole convergence, and a micro camera with the resolution of 225 pixels per inch (PPI) was placed inside the hollow platen of the Hoek cell for recording the borehole wall deformation during the testing and for its real-time visual monitoring. A 60 channel data acquisition system was connected to computers to monitor and record the axial force, axial displacement, axial

strain, lateral strain, convergence measurement and time into a storage device.

*2.2 Cut-off UCS*

Poorly cemented sandstones are characterized by low strength, poor cementation and high porosity (Bosio and Kanji, 1998). The UCS test results are generally considered for classification of weak sandstones from stronger hard rocks (ISRM 1981, He 2014 and Kanji 2014). In this study, Baud and Gambin (2011)'s approach for selecting the soft rocks based on the UCS upper limit of 10 MPa, as well as Liu and Wu (2016)'s guidance on classifying weak sandstone from stronger sandstone based on the UCS have been taken into consideration. To identify the mechanical properties a series of UCS tests were conducted on synthetic sandstones with various cement contents while keeping the water and sand components constant. Synthetic sandstone samples with four different cement contents, namely 10%, 12%, 14%, and 16% were considered for studying the effect of cement content on the UCS. These UCS tests were conducted based on the ISRM suggested methods (ISRM 1981) and under the same testing conditions.

Fig 1 a-c illustrate the compactor used to achieve uniform compaction of the specimen mixture in the mould, the synthetic rock specimens cast in the metal moulds, and the final solid synthetic specimens prepared for UCS testing respectively. The specimens were tested after 8 days of curing time and the average dry density was measured to be 1.79 g/cm$^3$.

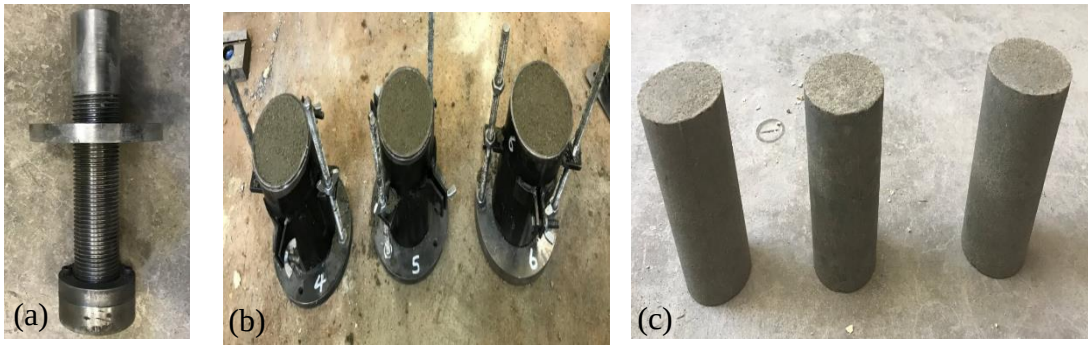


Fig 1. (a) Compactor, (b) Samples in the molds, (c) Unmoulded samples

The stress-strain diagrams obtained from the UCS tests are presented in Fig 2. The maximum

strength, $\sigma_{max}$ and the pre-maximum stiffness increase as the cement content increases. This trend is in agreement with the UCS test results obtained by Hashemi et al. (2015) where a lower range of cement content between 5% and 8% were used. It was observed that an increase in the cement content resulted in a higher maximum strength which also matches closely with other studies conducted on the influence of cement content on the UCS of synthetic sandstone specimens (Bernabe et al. 1992 and Saidi et al. 2003).

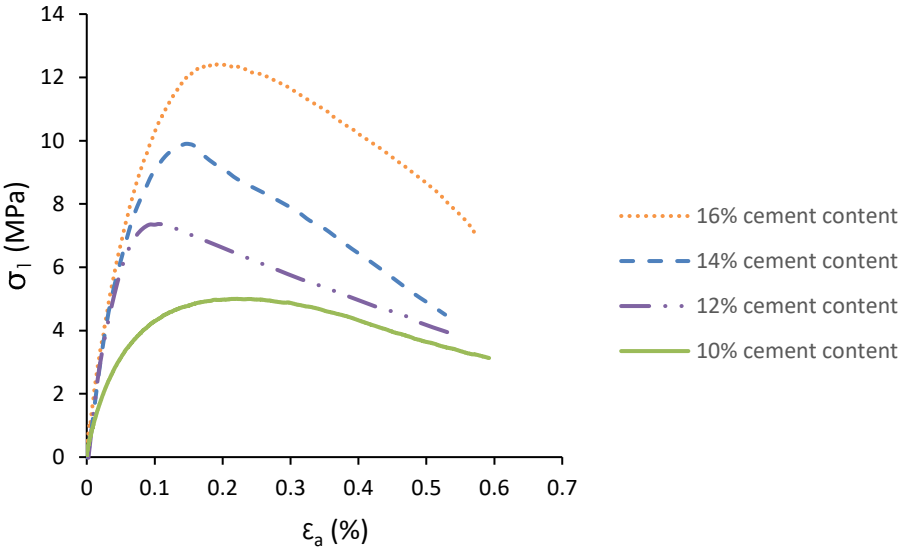


Fig 2. Stress versus axial strain behaviour for specimens subjected to UCS testing

As can be seen from Fig 2, the solid specimens with higher than 14% cement content exceeded the UCS of 10 MPa, therefore, 14% was identified as the upper cut-off cement content for this study, as increasing the cement content beyond this level resulted in a stronger specimen which does not meet the strength characteristic of a poorly cemented rock (Klein 2001). Three cementation levels (i.e. 10%, 12% and 14%) were considered for TWHC experiments.

### *2.3 Sample preparation and properties*

The sampling and preparation of natural poorly cemented sandstones for testing are usually very problematic due to difficulty in collecting undisturbed samples. As a result, sophisticated methods have been proposed by various researchers to make realistic synthetic poorly

cemented sandstone samples for testing (Saidi et al. 2003; Holt et al. 2005). Synthetic rock specimens are commonly used as an alternative for natural rocks for conducting laboratory-based borehole stability experiments (Younessi et al. 2012; Hashemi et al. 2015). The preparation of synthetic rocks involves mixing sand grains, a cementing agent and water. The mechanical properties of the prepared synthetic rock specimens depend on the individual components used in the mixture. A small variation in the initial components has a significant influence on the mechanical properties of the final specimens (Younessi et al, 2012). This indicates the importance of the careful selection of the components for the mixture. It has been observed that the mechanical properties of the synthetic rocks are primarily controlled by the cementation as grains are bonded together with a cementing agent (Saidi et al. 2003). Galvan and Kanji (2011) tested synthetic rock samples made under controlled conditions and found that the mechanical properties of the synthetic samples closely resembled those of the natural rocks.

To prepare synthetic sandstone samples with reasonably homogeneous properties, it is important to establish and follow a consistent sample preparation procedure. The synthetic sandstone specimens used in this study were prepared according to the mixture preparation procedure for a poorly cemented formation proposed by Hashemi et al. (2015). The mixture was composed of natural silica sands with two different grain size ranges, namely, coarse grain sands with a grain size between 0.425 mm-1.4 mm, and fine grain sands with a grain size between 0.15 mm-0.355 mm, Portland cement type II (specific gravity, $Gs$ = 3.15 $g/cm^3$) and water. The components were thoroughly mixed together to achieve a homogeneous mixture for specimens, and the time spent between pouring water into the dry mixture and compacting it into metal molds was maintained to be within 30 minutes to avoid initial setting of the cement. Each sample was prepared by compacting the mixture into three equal layers of 42 mm thickness. The top surface of the bottom layer was scratched before the subsequent layer was

compacted on top of it to ensure thorough interlocking between the successive layers. The mixture was not strong enough to bond sand grains in the early curing stage. Thus, the samples were left in the mould for five days, and then were removed from the mould and cured for another three days wrapped in a plastic film at room temperature (18-23°C) before testing. Mechanical properties of the specimens are presented in Table 1.

Table 1 Mechanical properties of the synthetic specimens

| Cement content (%) | Uniaxial Compressive Strength (MPa) | Poisson's ratio (ν) | Bulk density $\rho\ (\frac{kg}{m^3})$ |
|---|---|---|---|
| 10 | 4.96 | 0.243 | 1792 |
| 12 | 7.34 | 0.237 | 1859 |
| 14 | 9.90 | 0.231 | 1913 |

*2.4 Design of the CMD*

The convergence measuring device (CMD) is a simple mechanical device consisting of two strain gages attached to a V-shaped metal frame and positioned right opposite each other as is shown in Fig 3. Each strain gage is placed near the closed end of the metal frame where they exhibit the strain in compression or tension when the open ends of the CMD legs move. To allow a smooth contact with the borehole wall, round plastic bead is attached to each side of the outer surface of the CMD legs using a strong glue.

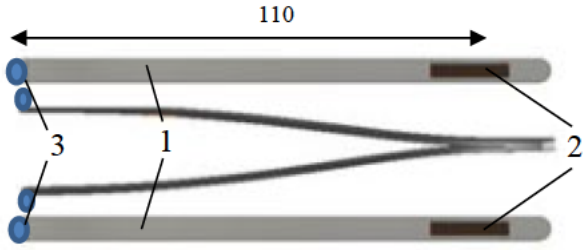


Fig 3. An illustration of components in a CMD 1. Metal frame, 2. Strain gage, 3. Plastic beads

The CMD was designed and developed with the primary focus on the contact based method, as the main purpose of the CMD is achieving an accurate measurement of the borehole

deformation in the TWHC specimens subjected to triaxial testing under various stress conditions. Non-contact based methods, such as the laser strain measurement device, were not considered due to the limited space inside a TWHC specimen not allowing to place such devices. The CMD is manufactured to be compact enough to be deployed inside a TWHC specimen with a small borehole size of 15 mm. The shape of the CMD was designed to allow for it be freely moved in and out of the borehole, and the dimensions of the metal frame were selected based on the size of the TWHC specimens to be tested. The key advantages of the proposed CMD are in its relatively simple manufacturing process, and in the versatility of its size, i.e. it can be manufactured in any size required to fit the specimen under consideration.

The working principle of the CMD is such that, when the borehole of the TWHC specimen is deformed under triaxial stress conditions, the movement of the CMD legs triggers either increase or decrease in the gage strain depending on the applied stress paths. The measurements taken from the two strain gages are then averaged and converted to displacement measurement through a calibration process; by co-relating the CMD leg displacement and the output from the strain gages. The strain gage currently in use has a resistance of 120 ohms with a grid dimension of 2.5 mm wide and 10 mm long (TML FLA-10-11). The two strain gages form a half Wheatstone bridge to enhance measurement accuracy and minimize the temperature effect.

### *2.5 Calibration of the CMD*

The calibration of the CMD was carried out by comparing and modifying the electrical value output from the strain gage versus the displacement output from the digital calibrator. The initial distance between the open ends of the CMD was set at 15 mm which matches the borehole diameter of the TWHC specimens. Both the CMD and the digital calibrator readings were zeroed for the initial measurement and then subsequent measurements were taken at every 0.1 mm displacement as the distance between the CMD legs was contracted by 0.1 mm at a step to its full range capacity. A digital micrometer (Mitutoyo digimatic micrometer 164), as

shown in Fig 4, with a resolution of 0.01 mm was used to get reference measurements for the calibration of the CMD. The calibration was carried out by comparing the measurements from the CMD and the digital micrometer output versus time.

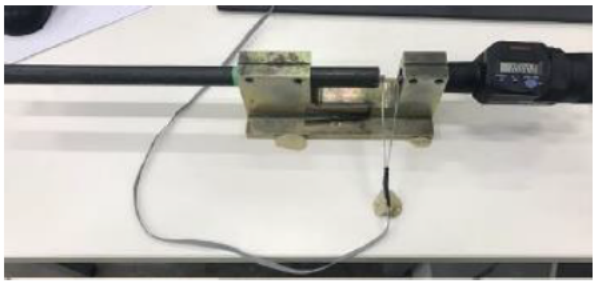

Fig 4. Digital micrometer and calibration set-up

Fig 5 presents the calibrated CMD output where the displacement matches closely with the calibrator output. Furthermore, to investigate the influence of the surface roughness on CMD reading several sensitivity tests were conducted on different types of surface materials in addition to the synthetic rocks. The results showed a consistent CMD reading for different types of surface materials.

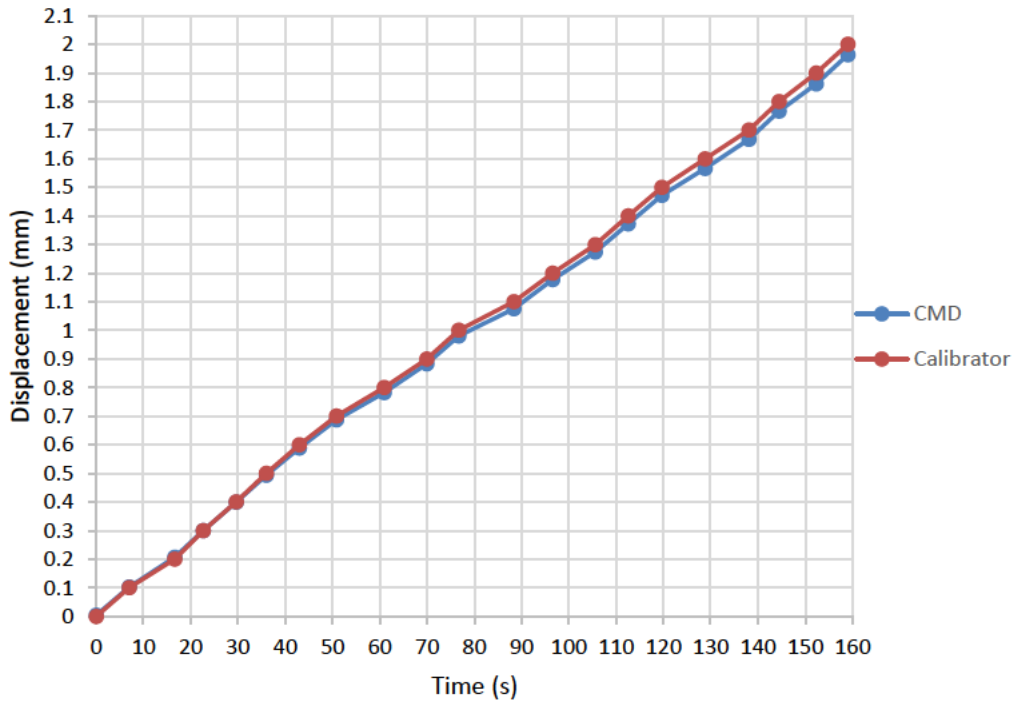


Fig 5. The CMD output from the calibration tests

*2.6 Experiment setup and procedure*

A modified Hoek cell designed and manufactured by Hashemi and Melkoumian (2016) consisting of two sets of cylindrical platens was used for conducting the TWHC tests. A micro camera was fitted inside the test cell to monitor and record the borehole wall in real-time. The Hoek cell was synchronized with a pressure maintainer specifically tuned for applying a low confining pressure without leakage. The CMDs were placed inside the TWHC specimen as shown in Fig 6a. A hollow cylindrical metal spacer made from hardened steel matching the diameter of the TWHC specimen was placed in between the specimen and the hollow platen to maintain the CMD in the vertical position during testing. A total of two CMDs were used for each test to improve the accuracy of the convergence measurement. The top CMD was placed alongside the camera and approximately 42 mm from the top end surface of the specimen, and the bottom CMD was placed on the direct opposite location of the top CMD.

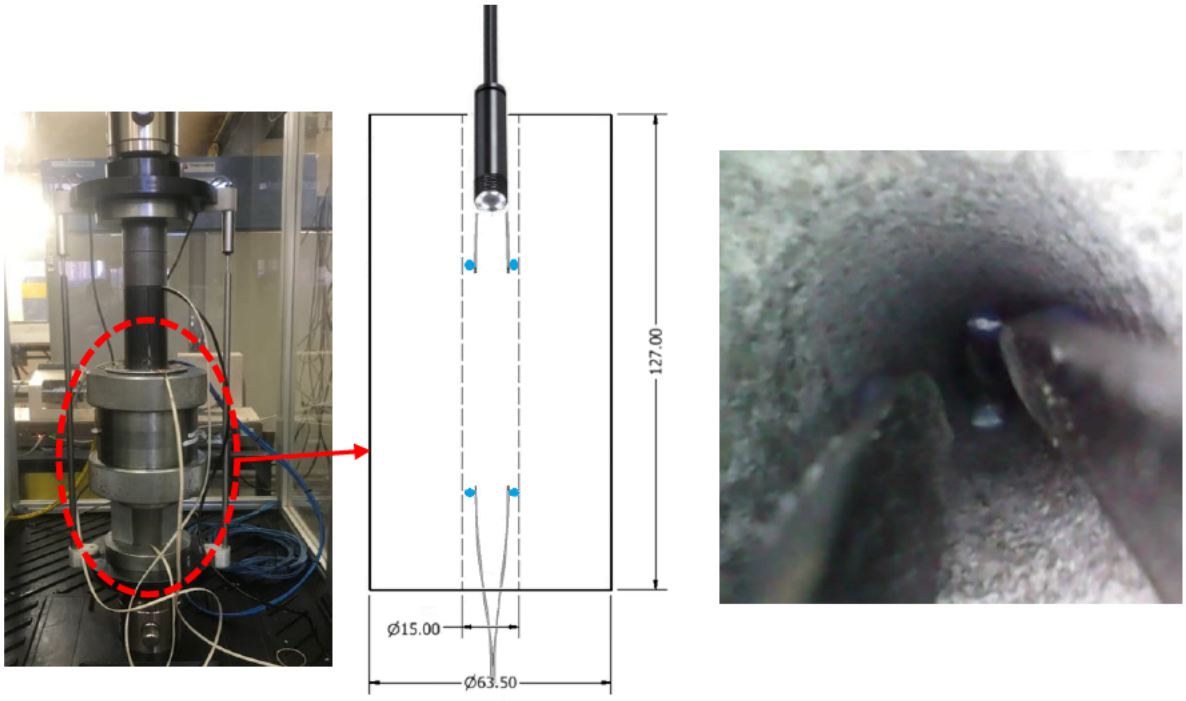


Fig 6. (a) The CMDs placed inside the Hoek cell and (b) the view from the micro camera

The end surfaces of each specimen were prepared to be flat and parallel to each other by applying a thin layer of dental paste. Lubrication was applied on the end surfaces in order to

minimize the friction between the platen and the specimen. Furthermore, spherical platens were placed on top of the hollow platen to ensure that uniform vertical stress is applied onto the TWHC specimen during testing and to minimize the bedding error. A pair of axial and lateral strain gages were attached directly to the sample surface to measure local deformations. A small load of approximately 5 N was applied by the loading machine as the top ram was lowered down to the surface of the platen prior to the commencement of the test to ensure full contact between the top ram and the platen. The image captured by the micro camera as shown in Fig 6b was checked for the clear focal point of the camera and to ensure that the CMDs were positioned vertically. The experiments were performed in two loading stages. In the first stage, simultaneous vertical and confining stresses were applied up to a pre-defined stress level to simulate the hydrostatic stress condition in the first stage of loading; and the second stage followed by increasing the vertical load at a constant displacement rate of 0.07 mm/min. The confining pressure was varied in each test to apply the desired confining stress to the TWHC specimen.

# 3. Results and discussion

### *3.1 UCS test results on solid specimens*

The UCS test results showed that the maximum strength and the pre-maximum stiffness increase as the cement content was increased. The influence of cement content on the peak strength was substantial. The UCS increased by 48% when the cement content was increased from 10% to 12%. Further increases in the cement content to 14% and 16% resulted in 35% and 25% increase in the UCS respectively, indicating that the influence of the cement content on the maximum strength becomes less significant as the cement content increases. This can be caused by the reduction in the grain to grain space available for cementation due to the increased cement content which pushes grains closer. Furthermore, according to Chen and Wu (2013), low water to cement ratio results in decreased cement hydration. Thus, the increase in

the cement content for the same water content could also have contributed to the reduced cement hydration due to excess cement particles not reacting with water. Laboratory studies by Saidi et al. (2003) also observed that in granular materials adding an additional cementing agent to the specimens with a low cement content of less than 20% is more likely to significantly increase their maximum strength, than adding a more cementing agent to the specimens with a higher cement content. The post-peak stress-strain trend of samples with 10 % cement content showed a greater ductile behaviour compared to the samples with a higher cement content of 12% and 14%. Moreover, the effect of water content was studied by varying the amount of water content between 10% and 12% while keeping other components unchanged. The increase in the water content resulted in strength reduction as a result of the increased total porosity. This outcome is in agreement with previous studies by Hashemi et al. (2015) conducted on synthetic sandstones with 10% water content.

*3.2 Triaxial test results on solid specimens*

Triaxial tests were carried out on solid cylindrical specimens with three different cement contents based on the preliminary UCS test results. Specimens with cement contents of 10%, 12%, and 14% were tested under different stress conditions. Fig 7a-c present the deviatoric stress ($\sigma_{deviatoric} = \sigma_1 - \sigma_{hydrostatic}$) versus the axial strain diagram for solid specimens with different cement contents. According to the results, an increase in the cement content and confining pressure resulted in the increase in the peak strength and the stiffness of the specimens as seen from the UCS tests. The specimens showed strain hardening behaviour and the material behaved non-linearly in the early stage of the loading processes. The non-linearity could be due to the rearrangement of sand particles leading to the closure of microcracks as the stress level was increased. Khan, Xiang, and Huang (1991) also observed such nonlinear behaviour in triaxial compression experiments using weak Berea sandstone. Hashemi et al. (2015) showed that the peak strength and ductility increase with the increase in the confining

pressure. As shown in Fig 7a-c, increasing the confining pressure results in the transition from the brittle to ductile behaviour. The ductility of specimens at a lower confining pressure of 2 MPa is less significant than at higher confining pressures of 4 MPa and 6 MPa.

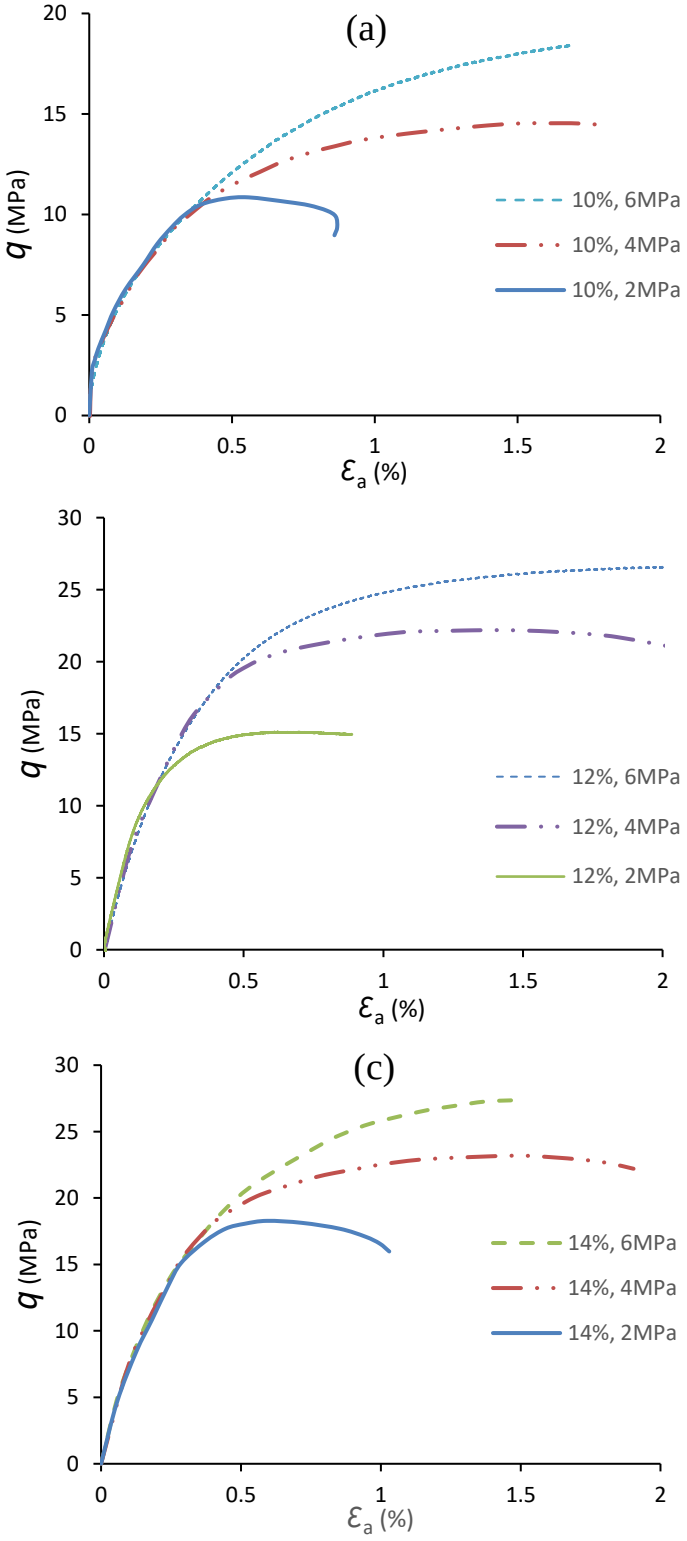


Fig 7. Deviatoric stress versus axial strain behaviour of solid specimens subjected to triaxial testing, (a) 10 % cement content, (b) 12 % cement content, (c) 14 % cement content

*3.3 Triaxial tests on thick-walled hollow cylinder specimens*

Triaxial tests were conducted on TWHC specimens with 15 mm diameter borehole for three different cement contents (10%, 12%, and 14%) and various confining pressures. As shown in Fig 8a-c, increasing the confining pressure by 2 MPa, increases the level of the peak strength and strain by up to 20 %. The pre-peak stiffness does not change dramatically with an increase in the confining pressure. However, for greater than 4 MPa of confining pressure, the increment in the level of strength is lower than that for the previous confining pressure of 2 MPa. For higher than 6 MPa of confining pressures the borehole collapsed prior to reaching the hydrostatic stress and, consequently, the strain gages on the specimens failed due to the weak surface of the specimen. Also, increasing the cement content while keeping the other parameters unchanged for sample preparation and test condition, increased the stiffness of the specimens.

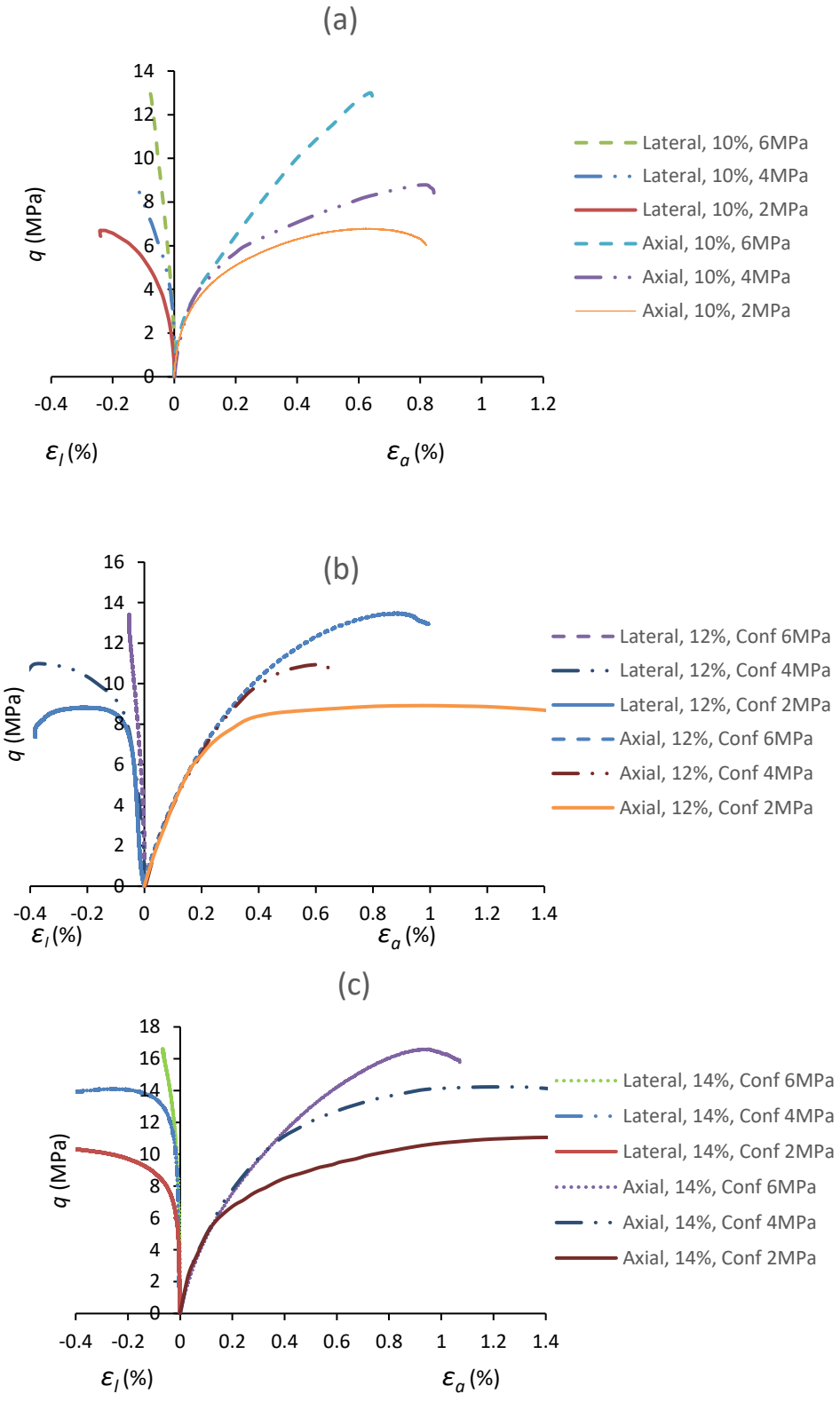


Fig 8. Deviatoric stress versus axial strain for TWHC specimens: (a) 10 % cement content, (b) 12 % cement content, (c) 14 % cement content

In the TWHC tests, a micro camera was used for real-time monitoring of the borehole. Visual monitoring of the borehole enabled identifying the location and shape of the borehole breakout

areas. Fig 9 a-d show the process of the borehole breakout captured by the camera during the axial loading test on a THWC specimen with 14 % cement content under 4 MPa of confining pressure. The borehole breakout took place in the form of a concentrated shear band around the borehole perimeter near the midpoint of the TWHC specimen as highlighted by the red circle. This result agrees with Papamichos' (2010) findings, who observed toroidally shaped shear band forming around the borehole during axial loading in a hollow cylinder test. The change in the borehole diameter was calculated by averaging the measurements taken by the two CMDs. The average borehole diameter measured by the CMDs at three different stages during the process of borehole breakout were 0.28 mm for Fig 9 (b), 0.52 mm for Fig 9 (c) and 0.97 mm for Fig 9 (d).

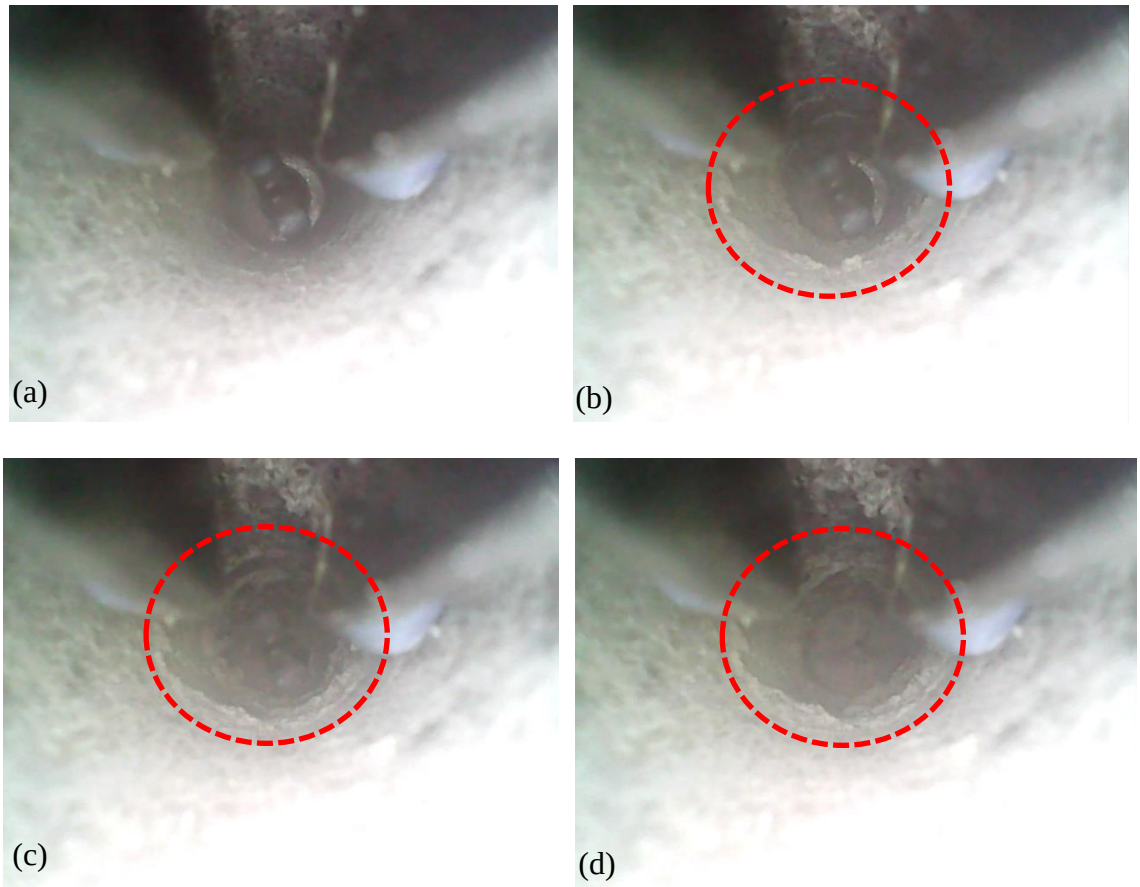


Fig 9. Borehole breakout captured by the micro camera

The test results obtained from the CMDs during the TWHC tests for three different cement contents at various confining pressures are shown in Fig 10a-c. The specimens were loaded

until borehole failure was observed from the video camera placed inside the borehole of the TWHC specimen. The deviatoric stress is plotted versus the borehole radial strain measured by the CMDs.

The stress-strain response of the TWHC specimen with 10% cement content in Fig 10a shows a constant increase in the radial strain as the borehole diameter converged gradually due to axial loading. The radial strain was initially 0%, but with the increasing stress, the radial strain increased. This is due to the compressive stress, which leads to material plastification, borehole convergence, and eventually borehole failure. The radial strain of the borehole increased at a faster rate once the borehole convergence was initiated. An increase in the confining pressure from 2 MPa to 6 MPa had a minimal effect on the change in the radial strain rate. A higher peak strength was observed for specimens tested under a higher confining pressure of 6 MPa compared to the specimens tested at lower confining pressures. This is in agreement with the experimental observations by Papamichos et al. (2010).

Fig 10b and Fig 10c present the results from the specimen with a higher cement content of 12% and 14% respectively. The stress-strain behaviour of the TWHC specimens tested under 6 MPa was similar to that for the specimens with a lower cement content of 10%. A different behaviour was observed for the specimens with 10% and 12% cement contents tested under a confining pressure of 4 MPa, as can be seen in Fig. 10b. The radial strain decreased prior to the initiation of the borehole failure, and this is due to the higher level of axial stress resulting in the expansion of the borehole at the contact point with the CMD devices. Prior to the initiation of the borehole break out, the radial strain increased as a relatively linear function of the deviatoric stress, as can be seen in Fig 10b-c. A constant increase in the radial strain was observed once the borehole breakout initiated.

The radial strain of the specimens with a higher cement content of 12 % and 14 % tested under various lateral confining pressures changed less significantly prior to the initiation of the

borehole failure compared to the specimens with a lower cement content of 10%. As shown in Fig 10a, the radial strain of the specimens with 10% cement content increases at a relatively steady rate up to 0.1%. After this point, the radial strain increases at a faster rate, indicating that the borehole diameter began to converge. However, Fig 10b-c show that the radial strain of the specimens with 12% and 14% cement contents tested under 2 MPa and 4 MPa of confining pressures changed less significantly prior to the rapid increase in the radial strain being observed once a specific radial strain was reached, indicating the collapse of the borehole wall when a critical deviatoric stress was applied. The specimens tested under a higher confining pressure of 6 MPa demonstrated a more gradual borehole convergence process as indicated by the constant increase in the radial strain compared to the specimens tested at a lower confining pressure. The results also showed that the increase in the cement content significantly influenced the deviatoric stress required to initiate the borehole convergence. However, the increment in the level of the deviatoric stress required for the borehole convergence initiation decreased when a high confining pressure of 6 MPa was applied.

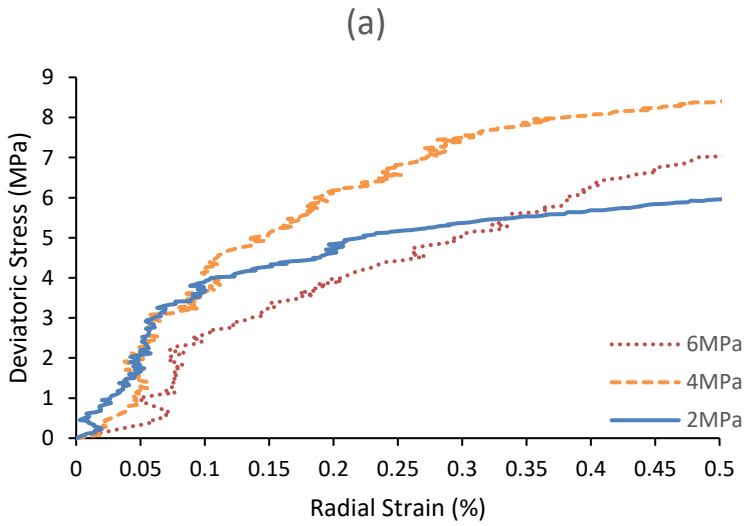

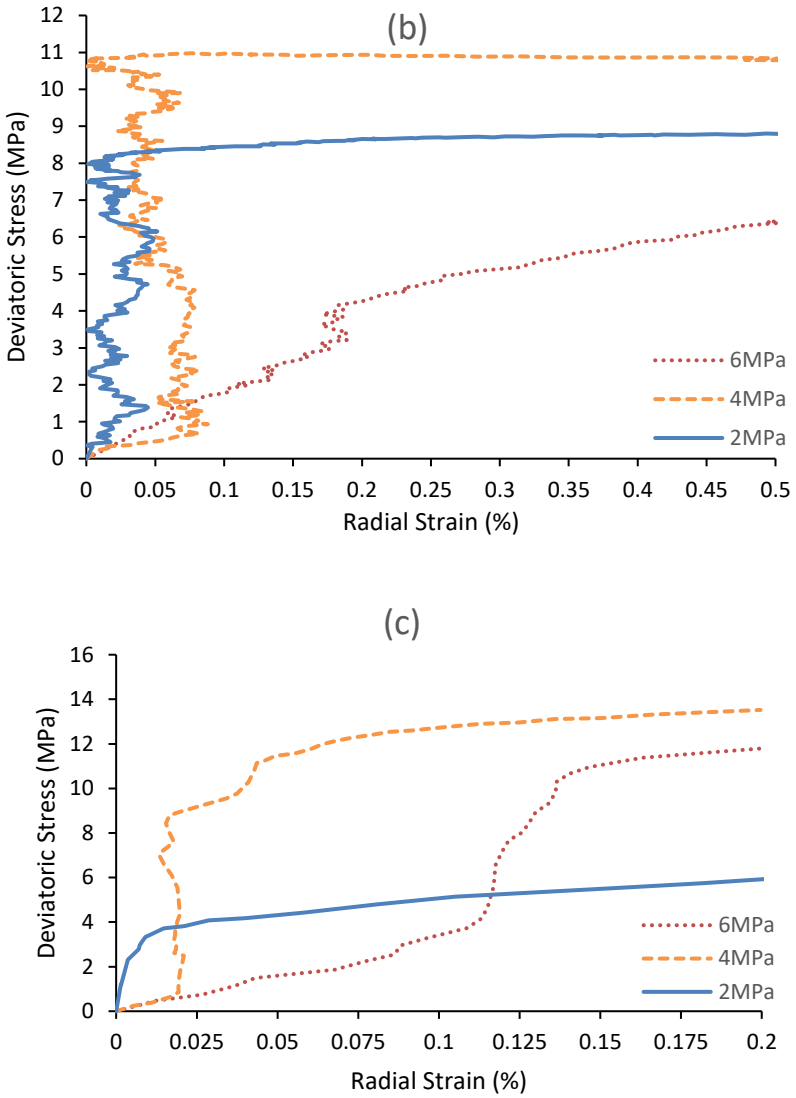


Fig 10. Deviatoric stress versus radial strain behaviour measured by the CMD for TWHC specimens subjected to triaxial testing: (a) 10 % cement content, (b) 12 % cement content, (c) 14 % cement content

# 4. Conclusions

A new laboratory-scale convergence measuring device was developed and applied in a series of laboratory experiments to measure the borehole deformation in TWHC specimens of synthetic poorly cemented sandstones with different amounts of cement contents. The results showed that the cement content and the magnitude of the lateral confining stress affect the borehole deformation behaviour and the failure stress.

In UCS tests, the maximum strength and pre-max stiffness increased with the increase in the cement content. However, the magnitude of increase in the maximum strength reduced as the cement content increased. The specimens with a lower cement content of 10% showed a greater ductility than the specimens with a higher cement content.

Triaxial test results showed a strain hardening behaviour with the increase in the cement content. The increase in the confining pressure resulted in the transition from a brittle to ductile behaviour. The peak strength and strain were largely influenced by the amount of the cement content. Also, it was observed that the increment in the level of the peak strength reduced as the confining pressure increased. The failure shape observed for the axial loading test was in the form of a shear band around the borehole wall, and the damage development and its localization into a shear band was successfully captured by the video camera placed inside the borehole of the TWHC.

The effect of the borehole deformation was investigated using the CMDs. The results showed that a relatively linear function of the deviatoric stress followed by a constant increase in the radial strain was observed as the borehole failure initiated. Prior to the initiation of the borehole failure, the radial strain of the specimens with a higher amount of cement content increased less dramatically compared to that for the specimens with a 10% cement content, indicating that the load-bearing capacity increases when the cement content is increased.

In summary, the presented experimental studies using the proposed CMDs have helped to gain a better understanding of the effects of the cement content and confining pressure on the borehole deformation behaviour and failure stress. Based on this finding, new drilling strategies

could be developed in the mining and petroleum industries to minimize borehole failures in poorly cemented sandy formations.

# 5. References


1. Al-Ajmi, A. and Zimmerman, R. (2006). Stability analysis of vertical boreholes using the Mogi–Coulomb failure criterion. International Journal of Rock Mechanics and Mining Sciences, 43(8), pp.1200-1211.
2. Baud JP, Gambin M. Classification of soils and rocks based on pressuremeter tests under high pressure. In: Proceedings of the 15th European Conference on Soil Mechanics and Geotechnical Engineering. Athens: Mill Press; 2011. pp. 325e30.
3. Bernabe, Y., Fryer D, & Hayes J. (1992) The effect of cement on the strength of granular rocks. *Geophys Res Lett*; 19:1511-1514.
4. Bosio JJ, Kanji MA. Soft rocks of the Rio de la Plata Basin. In: International Symposium on Indurated Soils and Soft Rocks, AGI, Naples. Rotterdam: A.A. Balkema;1998. pp. 65e71.
5. Bianco, P.M., and Halleck. (2001), Mechanisms of arch instability and sand production in two-phase saturated poorly consolidated sandstones, in SPE European Formation Damage Conference, the Hague, Netherlands
6. Bujok, P., Porzer, M., Labus, K., Klempa, M. and Pavluš, J. (2013). Experimental modeling of abandoned shallow oil wells convergence. *Engineering Geology*, 157, pp.1-7.
7. Chen X, Wu S. (2013). Influence of water-to-cement ratio and curing period on pore structure of cement mortar. *Construction and Building Materials*; 38:804-812
8. Fjar, E., Holt, R., Raaen, A., Risnes, R. and Horsrud, P. (2008). *Petroleum related rock*

*mechanics*. 2nd ed. Amsterdam: Elsevier, pp.309-310.

9. Galván V, Kanji MA. Simulation of arenaceous weak rocks by means of cemented sands. In: Proceedings of the 12th International Congress of International Society for Rock Mechanics. Beijing: CRC Press; 2011. pp. 751e2;
10. Goto, S., Tatsuoka, F., Shibuya, S., Kim, Y. and Sato, T. (1991). A simple gauge for local small strain measurements in the laboratory. *SOILS AND FOUNDATIONS*, 31(1), pp.169-180.
11. Hashemi, S.S, Melkoumian, N., Taheri, A. and Jaksa, M. (2015). The failure behavior of poorly cemented sands at a borehole wall using laboratory tests. *International Journal of Rock Mechanics and Mining Sciences*, 77, pp.348-357.
12. Hashemi S.S and Melkoumian N. (2016) Effect of different stress path regimes on borehole instability in poorly cemented granular formations. *Journal of Petroleum Science and Engineering*. 146:pp.30-49
13. Hight, D., Gens, A., and Symes, M. (1983). The development of a new hollow cylinder apparatus for investigating the effects of principal stress rotation in soils. *Géotechnique*, 33(4), pp.355-383.
14. Holt, R., Kjølaas, J., Larsen, I., Li, L., Gotusso Pillitteri, A. and Sønstebø, E. (2005). Comparison between controlled laboratory experiments and discrete particle simulations of the mechanical behavior of rock. *International Journal of Rock Mechanics and Mining Sciences*, 42(7-8), pp.985-995.
15. ISRM. (1981), Rock characterization, testing, and monitoring. ISRM suggested methods. International Journal of Rock Mechanics and Mining Sciences & Geomechanics Abstracts, 18(6), p.109.
16. Kanji, M. (2014). Critical issues in soft rocks. *Journal of Rock Mechanics and Geotechnical Engineering*, 6(3), pp.186-195.

17. Khan, A., Xiang Y. and Huang S. (1991) Behavior of Berea sandstone under confining pressure PART I: Yield and Failure Surfaces, And Nonlinear Elastic Response. *International Journal of Plasticity*, Vol. 7, pp.607-624.
18. Klein (2001). 'An approach to the classification of weak rock for tunnel projects' in Proceedings Rapid Excavation and Tunneling Conference. San Diego.
19. Li, SJ, Feng, X-T & Hudson, JA (2012), 'ISRM Suggested Method for Measuring Rock Mass Displacement Using a Sliding Micrometer', *Rock Mechanics and Rock Engineering*, vol. 46, no. 3, pp. 645-653.
20. Liu, K. and Wu, B. (2016). Predicting Reservoir Rock Mechanical Properties Directly from Sedimentary Characterisation. In: *SPE Asia Pacific Oil & Gas Conference and Exhibition*. Perth: Society of Petroleum Engineers.
21. O'Kelly B.C. and Naughton P.J. (2008). Use of proximity transducers for local radial strain measurements in a hollow cylinder apparatus. In: *Proceedings of the Fourth International Symposium on Deformation Characteristics of Geomaterials, Atlanta, Georgia, USA, 21st -24th September 2008*
22. Papamichos E, Liolios, P., and van den Hoek, P.J. (2004). Breakout stability experiments and analysis. In: 6th North America Rock Mechanics Symposium. Houston: American Rock Mechanics Association.
23. Papamichos E, Tronvoll J, Skjaerstein A, Unander TE (2010) Hole stability of red wildmoor sandstone under anisotropic stresses and sand production criterion. J Pet Sci Eng 72:78–92
24. Rawlings, C., Barton, N., Bandis, S., Addis, M. and Gutierrez, M. (1993). Laboratory and Numerical Discontinuum Modeling of Wellbore Stability. *Journal of Petroleum Technology*, 45(11), pp.1086-1092.
25. Saidi, F., Bernabe, Y. & Reuschle, T. (2003). The mechanical behavior of synthetic,

poorly consolidated granular rock under uniaxial compression. *Tectonophysics*, 370, pp.105-120.

26. Tronvoll, J. (1991). Experimental investigation of perforation cavity stability. *International Journal of Rock Mechanics and Mining Sciences & Geomechanics* Abstracts, 30(2), pp.365-373.
27. Wu, B., Chen, Z. and Zhang, X. (2016). Stability of Borehole with Breakouts - An Experimental and Numerical Modelling Study. In: 50th US Rock Mechanics/Geomechanics Symposium. Houston: American Rock Mechanics Association
28. Zhu, X. and Liu, W. (2013). The effects of drill string impacts on wellbore stability. *Journal of Petroleum Science and Engineering*, 109, pp.217-229.

# Chapter 2

# Evaluating the Effect of Different Stress Path Regimes on Borehole Deformation Using Convergence Measuring Device

# (Journal Paper 2, Published)

Jun Hyuk Heo, Noune Melkoumian and Sam S. Hashemi

School of Civil, Environmental and Mining Engineering

The University of Adelaide, SA 5005, Australia

Publication:

Heo, J. H., Melkoumian, N. & Hashemi S.S. (2022). Evaluating the Effect of Different Stress Path Regimes on Borehole Deformation using Convergence Measuring Device. *Geosciences, 12(9), 317*

# Statement of Authorship

| | |
|---|---|
| Title of Paper | Evaluating the Effect of Different Stress Path Regimes on Borehole Deformation using Convergence Measuring Device |
| Publication Status | ☑ Published ☐ Accepted for Publication ☐ Submitted for Publication ☐ Unpublished and Unsubmitted work written in manuscript style |
| Publication Details | Heo JH, Melkoumian N, Hashemi SS. Evaluating the Effect of Different Stress Path Regimes on Borehole Deformation Using Convergence Measuring Device. Geosciences. 2022; 12(9):317. |

## Principal Author

| | |
|---|---|
| Name of Principal Author (Candidate) | Jun Hyuk Heo |
| Contribution to the Paper | Performing laboratory tests, data analysis, writing and editing of the manuscript |
| Overall percentage (%) | 70% |
| Certification: | This paper reports on original research I conducted during the period of my Higher Degree by Research candidature and is not subject to any obligations or contractual agreements with a third party that would constrain its inclusion in this thesis. I am the primary author of this paper. |
| Signature | Date 02/09/2022 |

## Co-Author Contributions

By signing the Statement of Authorship, each author certifies that:

i. the candidate's stated contribution to the publication is accurate (as detailed above);

ii. permission is granted for the candidate in include the publication in the thesis; and

iii. the sum of all co-author contributions is equal to 100% less the candidate's stated contribution.

| | |
|---|---|
| Name of Co-Author | Dr. Noune Melkoumian |
| Contribution to the Paper | Conceptulisation, supervision and review of the manuscript |
| Signature | Date 25.09.2022 |

| | |
|---|---|
| Name of Co-Author | Dr. Sam S. Hashemi |
| Contribution to the Paper | Methodology, Supervision and review of the manuscript |
| Signature | Date 02/09/2022 |

Please cut and paste additional co-author panels here as required.

# Abstract

A laboratory study was conducted to investigate the borehole deformation of poorly cemented sandstone rocks with Uniaxial Compressive Strength (UCS) less than 10 MPa under different stress path regimes by using a convergence measuring device (CMD). Synthetic thick-walled hollow cylinders (TWHCs) comprised of sand grains, Portland cement and water were prepared for this study. A series of mechanical tests including uniaxial and triaxial compression tests were performed to examine the physical properties of the artificial sandstones. The CMD was deployed inside the TWHC specimen to measure the borehole deformation. Five different stress paths were applied to the specimens to investigate the effect of stress paths and three different cement agent contents (10%, 12% and 14%) were considered to study the effect of cement content on the borehole failure. The effect of the cement content on the borehole failure was found to be more significant than the effect of change is stress path regimes.



Keywords: Borehole deformation; convergence measuring device; thick-walled hollow cylinder; borehole monitoring


# 1. Introduction

Drilling boreholes and creating other cavities in the ground disturbs the local in situ stress field due to the stress concentration around the cavity. Under the stress concentration, weak bonding between the particles in poorly cemented formation may break when there is an inadequate cement agent present between the interfaces of sand grains. Leading to inelastic damaged zone and borehole failure. Understanding the responses of poorly cemented formation is important for the prediction of failure modes and mechanical characteristics. Borehole convergence is a fundamental parameter in borehole stability analysis involving

deformational calculations. In order to ensure long term stability of modern drilling operations, the acquisition of geotechnical information about encountered formation is critical for early detection of instability issues and minimizing borehole failure. While various convergence measuring devices such as caliper log, borehole extensometer, and convergence monitor are being used in the field, relatively few efforts have been made to accurately measure the borehole convergence in laboratory experiments for weak rocks under different stress path regimes. The cell of Bonnechere, the USBM gage and the CSIRO HI cell have been proposed for laboratory-based tests to measure the borehole deformation (Amadei and Stephansson, 1997). However, their application requires an extensive installation procedure and is limited to a specific borehole diameter size matching the size of the monitoring device, i.e. the diameter must be more than 30 mm. In the current study a cost-effective, versatile and reliable convergence measuring device with a quick and easy installation procedure was developed based on the concept of the LDT proposed by Goto et al. (1991) to evaluate the borehole deformation in thick-walled hollow cylinder specimens. These new CMDs have been calibrated and tested in laboratory conditions in order to verify their performance under different stress paths for poorly cemented sands.

Laboratory experiments involving the measurement of the diametric deformation of a borehole by placing a two-arm caliper inside a hollow cylinder were carried out by Tronvoll (1992). However, the effect of different stress paths was not investigated. Igarashi et al. (2008) developed a borehole tangential deformation gage to measure the tangential deformation of the borehole wall. Papamichos et al. (2010) performed laboratory experiments on hollow cylinder specimens of Red Wildmore sandstone where they used cantilever strain gage pairs to study the effect of the stress anisotropy on the borehole deformation. Bujok et al. (2013) conducted experimental studies on the effects of the well convergence on the deformational shape of the borehole. Wu et al. (2016) conducted polyaxial tests with a four-arm cantilever

borehole gage placed inside the borehole within a block specimen to measure the borehole deformation. These tests involved a relatively stronger sandstone with a uniaxial compressive strength (UCS) of greater than 10 MPa.

Laboratory experiments are found to be one of the most effective methods for studying the borehole failure mechanism. An experimental study on the effect of borehole inclination was conducted by Rawlings et al. (1993) using both synthetic and natural weak sandstone specimens. Haimson and Song (1998) observed a deep and narrow 'slot' shaped breakout in poorly cemented sandstone from a TWHC test. Papamichos et al. (2010) studied the effect of anisotropic stress paths on weak natural sandstone. Younessi et al. (2012a) conducted TWHC tests as well as true triaxial tests on synthetic sandstone specimens representing poorly cemented formations. Bujok et al. (2013) studied the effect of borehole convergence using a specially made pressure vessel by applying confining pressure onto a wellbore model consisting of different layers of rock materials. Hashemi et al. (2015) carried out TWHC tests on poorly cemented sands focusing on the effects of cement content, anisotropic stress paths and borehole sizes. Furthermore, limited available research conducted on borehole convergence measuring sensors that can be applied for laboratory based experimental studies indicate ae needs for the development of sensors that can accurately measure borehole convergence. Zhang and Liu (2019) demonstrated that the effect of confining pressure in the range of 2 ~13 MPa using hollow cylinder specimens on two different sandstones was nearly the same. Yan et al. (2020) recently conducted a comparative study between unconsolidated and weakly consolidated sandstones and concluded that weakly consolidated sandstones tended to develop localised failure whereas, unconsolidated sandstones failed uniformly.

This study aims to investigate the application of the CMD on monitoring borehole deformation under different stress path regimes. A series of laboratory based TWHC tests were designed and conducted under various stress paths. Both far-field and an element on the

borehole wall were considered for applying different stress paths. The borehole behaviour was monitored by a video camera to record borehole in order to determine the borehole failure along the borehole for the specimens. The results present a realistic understanding of the failure behaviour of poorly cemented sand formations under different stress paths.

# 2. Experimental Study

The Uniaxial Compressive Strength (UCS), triaxial and TWHC tests are the most widely used and versatile rock mechanics tests for determining the parameters required for borehole stability analysis and understanding the behaviour of a granular formation under different stress conditions. In this study, the borehole stability experiments were performed on TWHC specimens in a modified Hoek Cell. During each test, the CMDs were deployed inside the borehole of the TWHC specimen for measuring the borehole diameter convergence, and a micro camera with the resolution of 225 pixels per inch (PPI) was placed inside the hollow platen of the Hoek cell for recording the borehole wall deformation during the testing and for its real-time visual monitoring. The TWHC specimen was subjected to an axial stress along the borehole axis, and the confining stress was provided by a servo-controlled hydraulic device.

A number of laboratory facilities were used for conducting the tests. For applying vertical stress to the specimen, a servo controlled axial loading system of 300 kN capacity with 0.1 N accuracy was used. For applying and maintaining the external confining pressure at a very low level, the Hoek cell was connected to an automatic hydraulic machine which had a relief valve and a pressure gage with an accuracy of 0.01 MPa. A 60 channel data acquisition system was connected to computers to monitor and record axial force, axial displacement, axial strain, lateral strain, convergence measurement and time into a storage device.

*2.1 Laboratory testing*

The TWHC specimens were prepared in the laboratory under controlled conditions to manufacture poorly cemented sandstone specimens that resemble those of the natural rocks. Synthetic rock specimens are frequently used as an alternative to natural rocks for conducting laboratory-based borehole stability experiments (Younessi, Rasouli, and Wu 2013; Hashemi et al. 2015). The preparation of synthetic rocks involves mixing sand grains, a cementing agent, and water. The mechanical properties of the prepared synthetic rock specimens depend on the individual components used in the mixture. A small variation in the initial components has a significant influence on the mechanical properties of the final specimens (Younessi, Rasouli, and Wu 2013). This indicates the importance of the careful selection of the components for the mixture. It has been observed that the mechanical properties of the synthetic rocks are primarily controlled by the cementation as the sand grains are bonded together by a cementing agent (Saidi, Bernabe, and Reuschle 2003). Liévano and Kanji (2011) tested synthetic rock specimens made under controlled conditions and found that the mechanical properties of the synthetic specimens closely resemble those of the natural rocks.

Synthetic sandstone specimens which are close to the weak formations in terms of mechanical parameters such as the UCS are less than 10 MPa. For further experimental study of borehole convergence behaviour of this type of sandstone, other parameters such as high porosity and permeability were replicated. The synthetic sandstone specimens used for this study were prepared according to the mixture preparation procedure for poorly cemented formation proposed by Hashemi et al. (2015) to achieve homogeneous properties. The mixture was composed of natural silica sands with two different grain size ranges, namely, coarse grain sands with grain size between 0.425 mm and 1.4 mm, and fine grain sands with a grain size between 0.15 mm and 0.355 mm, Portland cement type II (specific gravity, $Gs$ = 3.15 $g/cm^3$) and water. The components were thoroughly mixed together to achieve a homogeneous

mixture for the specimens and the time spent between pouring water into the dry mixture and compacting it into metal moulds was maintained to be within 30 minutes to avoid initial setting of the cement. Each specimen was prepared by compacting the mixture into three equal layers of 42 mm thickness. The bottom surface between the layers was scratched before the subsequent layer was compacted on top to ensure thorough interlocking between the successive layers. The mixture was not strong enough to bond sand grains in the early curing stage. Thus, the specimens were left in the mould for five days, and then removed from the mould and cured for another three days wrapped in a plastic film at a room temperature (18-23°C) before testing. The opposite ends of the specimen are made perfectly parallel. Further details for specimen preparation can be found in Hashemi et al. (2015).

*2.2 Design of the CMD*

The convergence measuring device (CMD) was designed based on the local deformation transducer (LDT) developed at the Institute of Industrial Science, University of Tokyo (Goto et al. 1991). The LDT is a simple and low-cost device that is capable of accurately measuring axial strains to $10^{-4}$ %. The working principle of the CMD is such that, when the borehole of the TWHC specimen is deformed under triaxial stress conditions, the movement of the CMD legs triggers either increase or decrease in the gage strain depending on the applied stress paths. The measurements taken from the two strain gages are then averaged and converted to displacement measurement through a calibration process; by co-relating the CMD leg displacement and the output from the strain gages. The strain gage currently in use has a resistance of 120 ohms with a grid dimension of 2.5 mm wide and 10 mm long (TML FLA-10-11). The two strain gages form a half Wheatstone bridge to enhance measurement accuracy and minimize the temperature effect.

Fig 1 shows the final CMD manufactured for testing. It consists of strain gage attached to either side of a V-shaped metal frame that are positioned right opposite each other as shown below.

Fig 1. Convergence Measuring Device

Each strain gage is placed near the closed end of the metal frame where it exhibits the strain in compression or tension when the open ends of the CMD legs move. To allow a smooth contact with the borehole wall, a circular plastic bead was attached to each side of the outer surface of the CMD legs using a strong glue.

*2.3 Calibration of the CMD*

The calibration of the CMD was carried out by comparing and modifying the output from the strain gage versus the displacement output from the digital calibrator. The initial distance between the open ends of the CMD was set at 15 mm which matches the borehole diameter of the TWHC specimens. Both the CMD and the digital calibrator readings were zeroed for the initial measurement and then subsequent measurements were taken at every 0.1 mm displacement as the distance between the CMD legs was contracted by 0.1 mm at a step to its full range capacity. A digital micrometre (Mitutoyo digimatic micrometre 164) with a resolution of 0.01 mm was used to get reference measurements for the calibration of the CMD. The calibration was carried out by comparing the measurements from the CMD and the digital micrometre output versus time.

*2.4 Experimental devices and calibration*

A triaxial stress system (MTS) was used for the test. This system is capable of supplying, maintaining, monitoring and controlling confining pressure as well as measuring accurate radial and axial displacements. Hoek cell was used to maintain pre-defined confining pressure on the specimen. Hydrostatic loading was applied for each of the stress paths tested. In order to measure accurate volumetric strain measurement, two axial variable displacement transformers (LVDT) and strain gauges were used. For the UCS testing the specimens were prepared in three different cement contents to study the effect of cementing agent. UCS tests were conducted on the specimens of 65.3 mm in diameter and 127 mm in height.

A hollow cylinder test is used to apply an axial load and an external pressure along the curved surface of the cylinder specimen that provides a ready method for studying the strength. The modified Hoek cell designed and manufactured by Hashemi and Melkoumian (2016) consisting of two sets of cylindrical platens was used for conducting the TWHC tests. A micro camera was fitted inside the test cell to monitor and record the borehole wall in real-time. The Hoek cell was synchronized with a pressure maintainer specifically tuned for applying a low confining pressure without leakage. The CMDs were placed inside the TWHC specimen as shown in Fig 2a. A hollow cylindrical metal spacer made from hardened steel matching the diameter of the TWHC specimen was placed in between the specimen and the hollow platen to maintain the CMD in the vertical position during testing. A total of two CMDs were used for each test to improve the accuracy of the convergence measurement. The top CMD was placed alongside the camera and approximately 42 mm from the top end surface of the specimen, and the bottom CMD was placed on the direct opposite location of the top CMD.

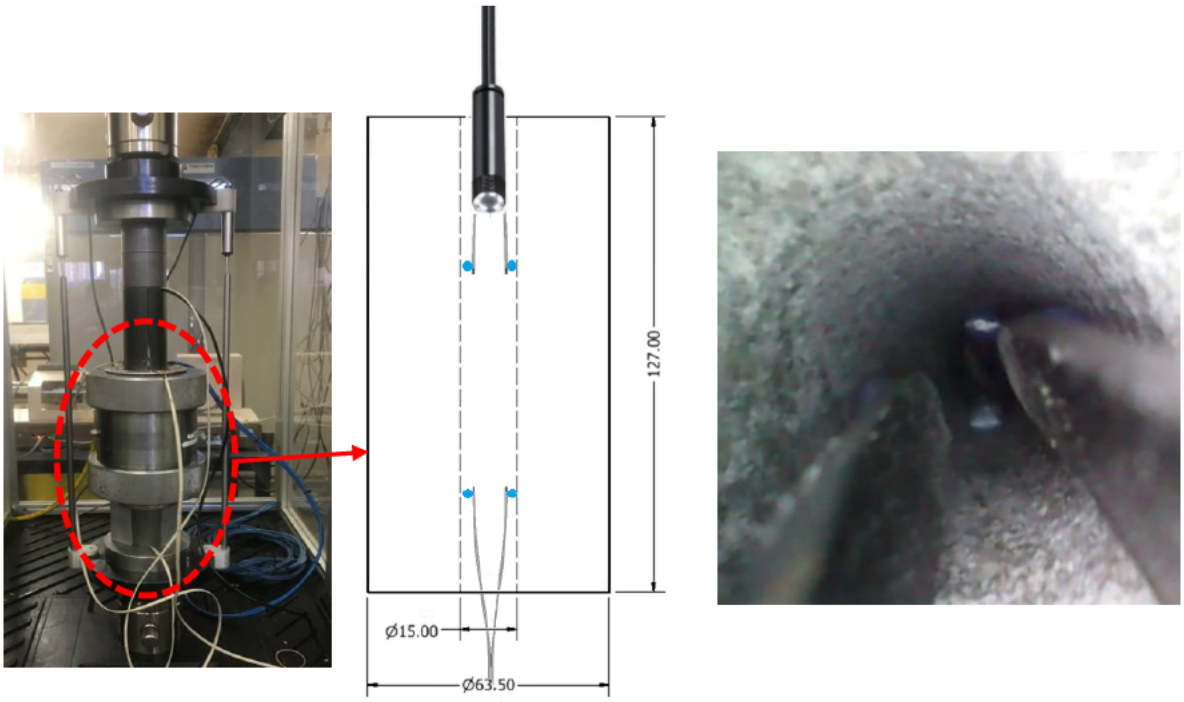


Fig 2. (a) The CMDs placed inside the Hoek cell and (b) the view from the micro camera

The end surfaces of each specimen were prepared to be flat and parallel to each other by applying a thin layer of dental paste. Lubrication was applied on the end surfaces in order to minimize the friction between the platen and the specimen. Furthermore, spherical platens were placed on top of the hollow platen to ensure that a uniform vertical stress was applied onto the TWHC specimen during testing and to minimize the bedding error. A pair of axial and lateral strain gages were attached directly to the specimen surface to measure local deformations. A small load of approximately 5 N was applied by the loading machine as the top ram was lowered down to the surface of the platen prior to the commencement of the test to ensure full contact between the top ram and the platen. The image captured by the micro camera as shown in Fig 2(b) was checked for the clear focal point of the camera and to ensure that the CMDs were positioned vertically. The experiments were performed with the following two loading stages; first, simultaneous vertical and confining stresses were applied up to a pre-defined stress level to simulate the hydrostatic stress condition in the first stage of loading. The second stage was followed by increasing the vertical load at a constant

displacement rate of 0.07 mm/min. Confining pressure was varied in each test to apply desired confining stress to the TWHC specimen. Fig 3 illustrates borehole convergence observed by the camera placed above the specimen during a TWHC test under the first stress path without the CMD placed inside the borehole. The camera captured three different stages of borehole convergence, Fig 3 shows sand particles beginning to dislodge followed by visibly deformed borehole and then the fully converged borehole.

Fig 3. Borehole convergence observed by the camera

*2.5 Stress paths*

The effect of stress paths on the behaviour of TWHC was investigated by applying five different stress paths. In the first stress path, hydrostatic condition was simulated on the boundary of the specimens by applying both the axial stress and the confining pressure simultaneously at the same rate up to the pre-defined value, Then, in the second step, an axial loading was applied at a constant displacement rate of 0.07 mm/min while constant confining pressure was being applied to the external surface of the specimens controlled by an automatic pressure gauge system. The second stress path was simulated by applying hydrostatic condition followed by applying a constant increase in confining pressure at a rate of 0.2 MPa/min to the specimens. In the third and fourth stress paths, $\sigma_{\theta} \approx \sigma_z$ the confining pressure value was derived in terms of the tangential stress.

$$
\begin{aligned}
&1^{st}\text{ stress path} \begin{cases} \sigma_1 = \sigma_2 = \sigma_3 = \sigma_{conf} = \sigma_z \text{(first step)} \\ \sigma_1 = \sigma_z > \sigma_2 = \sigma_3 = \sigma_{conf} \text{(second step)} \end{cases} && \text{(1a)} \\
&2^{nd}\text{ stress path} \begin{cases} \sigma_1 = \sigma_2 = \sigma_3 = \sigma_{conf} = \sigma_z \text{(first step)} \\ \sigma_1 = \sigma_2 = \sigma_{conf} > \sigma_3 = \sigma_z \text{(second step)} \end{cases} && \text{(1b)} \\
&3^{rd}\text{ stress path} \begin{cases} \sigma_1 = \sigma_2 = \sigma_\theta = \sigma_z > \sigma_3 = \sigma_r = 0 \text{(first step)} \\ \sigma_1 = \sigma_\theta = \sigma_2 = \sigma_z > \sigma_r = 0 \text{(second step)} \end{cases} && \text{(1c)} \\
&4^{th}\text{ stress path} \begin{cases} \sigma_1 = \sigma_2 = \sigma_\theta = \sigma_z > \sigma_3 = \sigma_r = 0 \text{(first step)} \\ \sigma_1 = \sigma_z > \sigma_2 = \sigma_\theta > \sigma_r = 0 \text{(second step)} \end{cases} && \text{(1d)} \\
&5^{th}\text{ stress path} \begin{cases} \sigma_1 = \sigma_\theta = \sigma_2 = \sigma_z > \sigma_r = 0 \text{(first step)} \\ \sigma_1 = \sigma_\theta = \sigma_2 = \sigma_z > \sigma_r = 0 \text{(second step)} \end{cases} && \text{(1e)}
\end{aligned}
$$

# 3. Results

*3.1 First Stress Path*

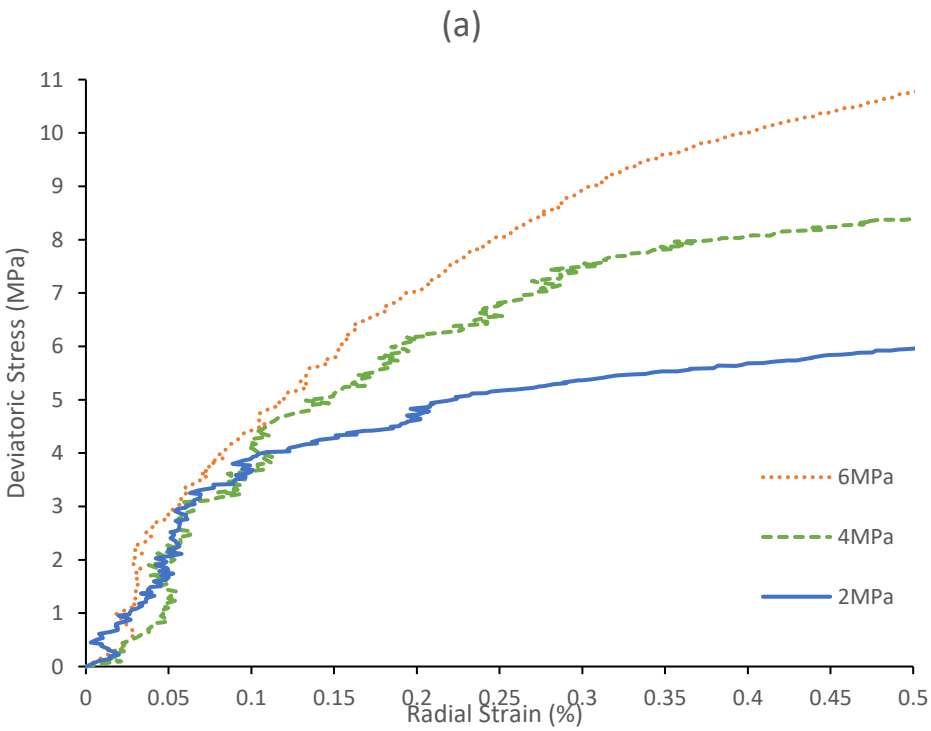

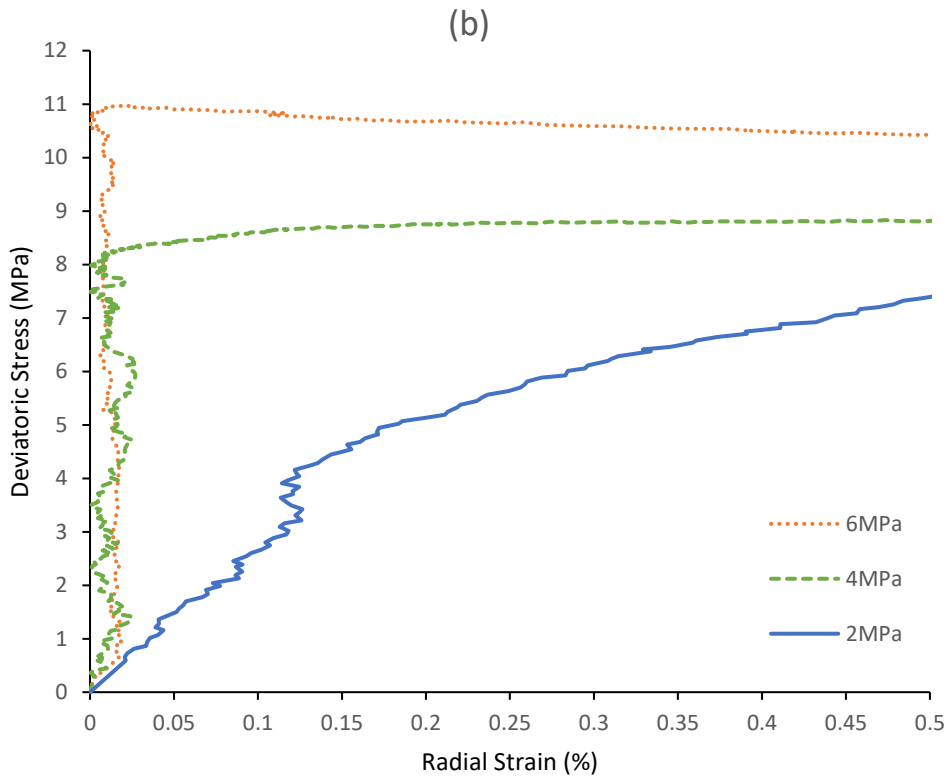


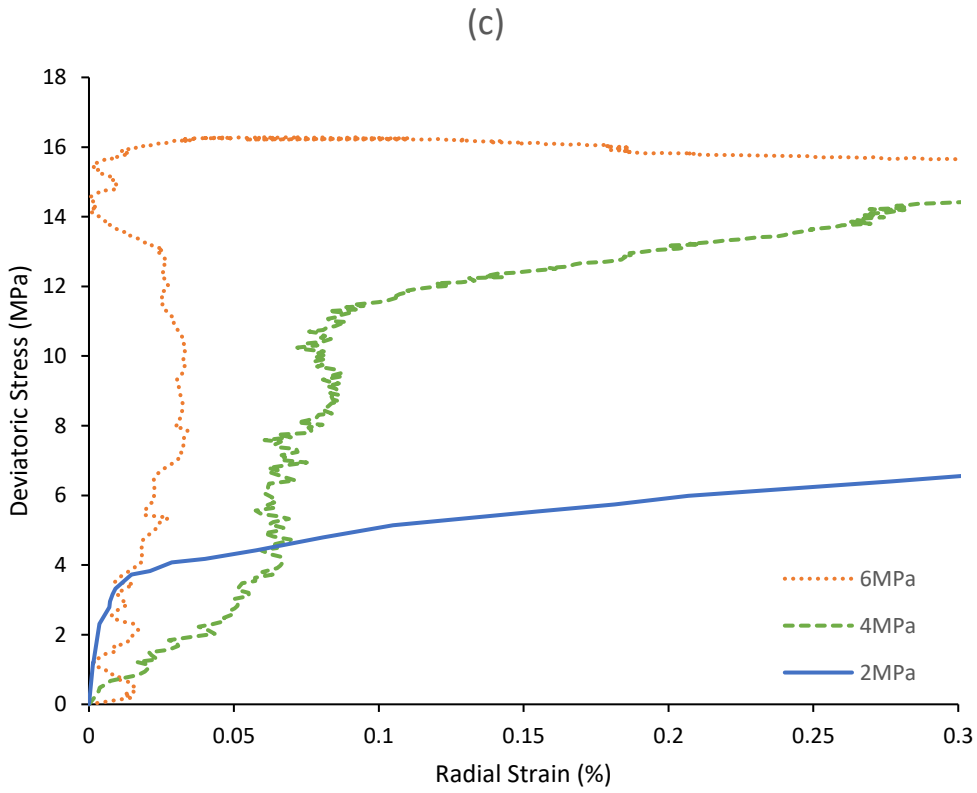


Fig 4. Deviatoric stress (MPa) versus radial strain (%): (a) 10% cement content, (b) 12% cement content, 14% cement content.

In the first stress path, both the axial stress and the confining pressure were increased simultaneously at the same rate up to the pre-defined level, in order to simulate hydrostatic condition on the boundary of the specimens. Then, in the second step, the specimen was subjected to an axial loading increment corresponding to a constant displacement rate of 0.07mm/min. During the test, the level of the confining pressure applied to the external surface of the specimens was kept constant by an automatic pressure gauge system. The results showed the relatively linear function of the deviatoric stress followed by a constant increase in the radial strain as the borehole failure initiated. This behaviour was more profound at a lower level of cement content of 10% compared to specimens with a higher cement content of 12% and 14%. Prior to the initiation of the borehole failure, the radial strain of the specimens with a higher amount of cement content increased less dramatically compared to that for the specimens with 10 % cement content, indicating that the load-bearing capacity increases when the cement content is increased. The specimens under the first stress path showed that borehole failure occurred in the strain-hardening section of the stress strain diagram, furthermore, increase in cement content increased the lateral stiffness of the specimen in the vertical direction.

*3.2 Second Stress Path*

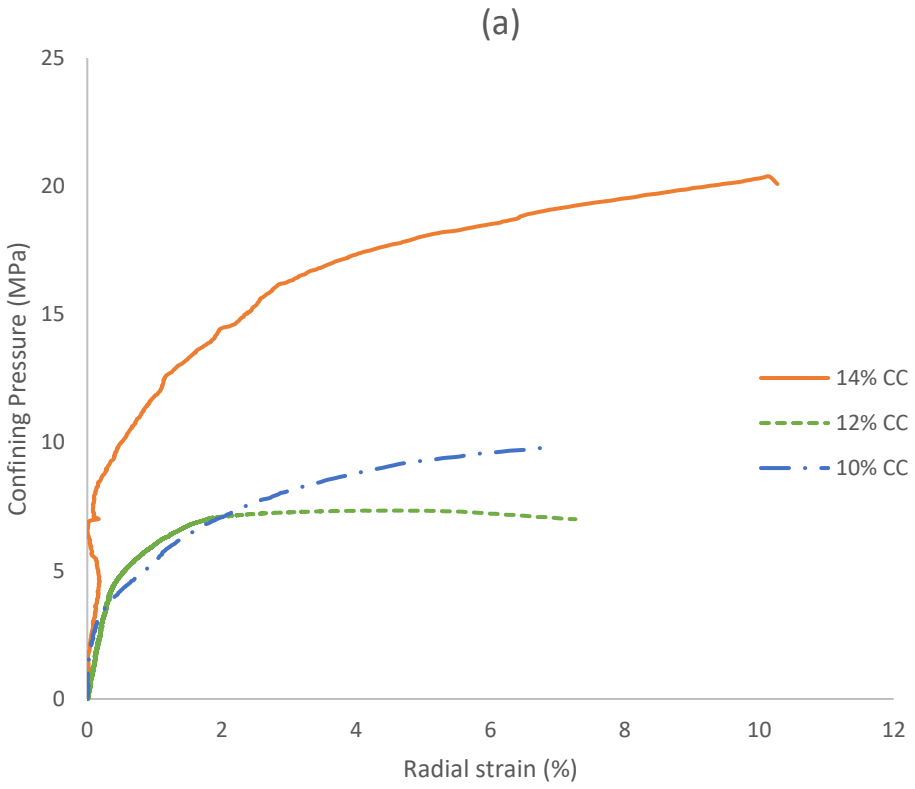


Fig 5. Confining pressure (MPa) versus radial strain (%)

The increase in the cement content had a minimal effect on the stiffness of the specimens tested under the second stress path. Mogi (2007) suggested that the stiffness depends on the rock material and, as the same sand grain sizes were used for the specimen preparation, the specimen stiffness remained unchanged in the tests. The level of the confining pressure required to initiate a borehole convergence increased with the increase in the cement content. This is due to the strengthening effect of the cement. Hashemi et al. (2015) have also observed that the poorly cemented specimens with a higher cement content demonstrate a higher peak strength due to the strengthening effect of the cementing agent. Generally, for the second path with an increase in the cement content, the radial strain increased for a certain confining stress. With increasing the cement content, the stiffness of the specimens in the vertical direction obtained higher values than in the lateral orientation for the second path however, the rate of increase was lower for the second path. Fig 5 shows that the effect of cement content has a

higher influence on stabilizing a borehole than that of the confining stress applied for the second stress path. The level of confining pressure required to initiated a borehole convergence increased with the increase in the cement content. Such observation agrees with Hashemi et al. (2015) where the poorly cemented specimens with a higher cement content demonstrated a higher peak strength due to the strengthening effect of the cementing agent. Fig 6 below illustrates the borehole failure process observed from the camera installed inside the borehole. Moreover, the specimens showed a more ductile behaviour when the equal amount of vertical stress and the maximum principal stress were applied to them. The borehole failure was observed at lower strains for the second path compared to the first path, which suggests that the tangential stress has the important influence on the borehole failure in poorly cemented specimens. Results displayed that the shear bands were formed, and the produced sand mainly consisted of uniform loose grains.

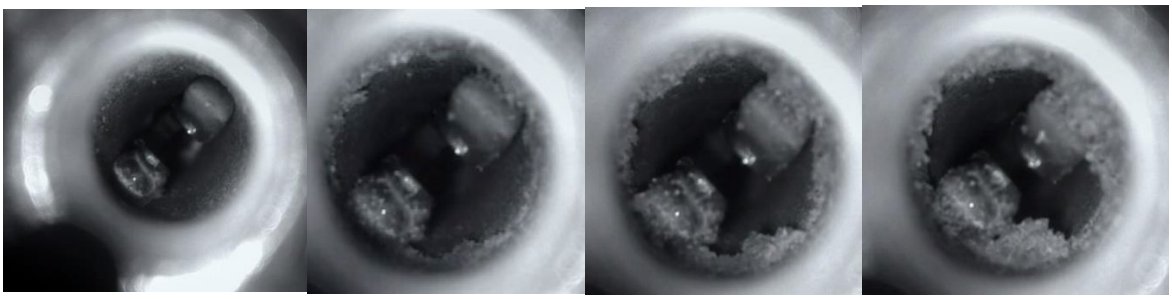

Fig 6. Borehole failure observations.

*3.3 Third Stress Path*

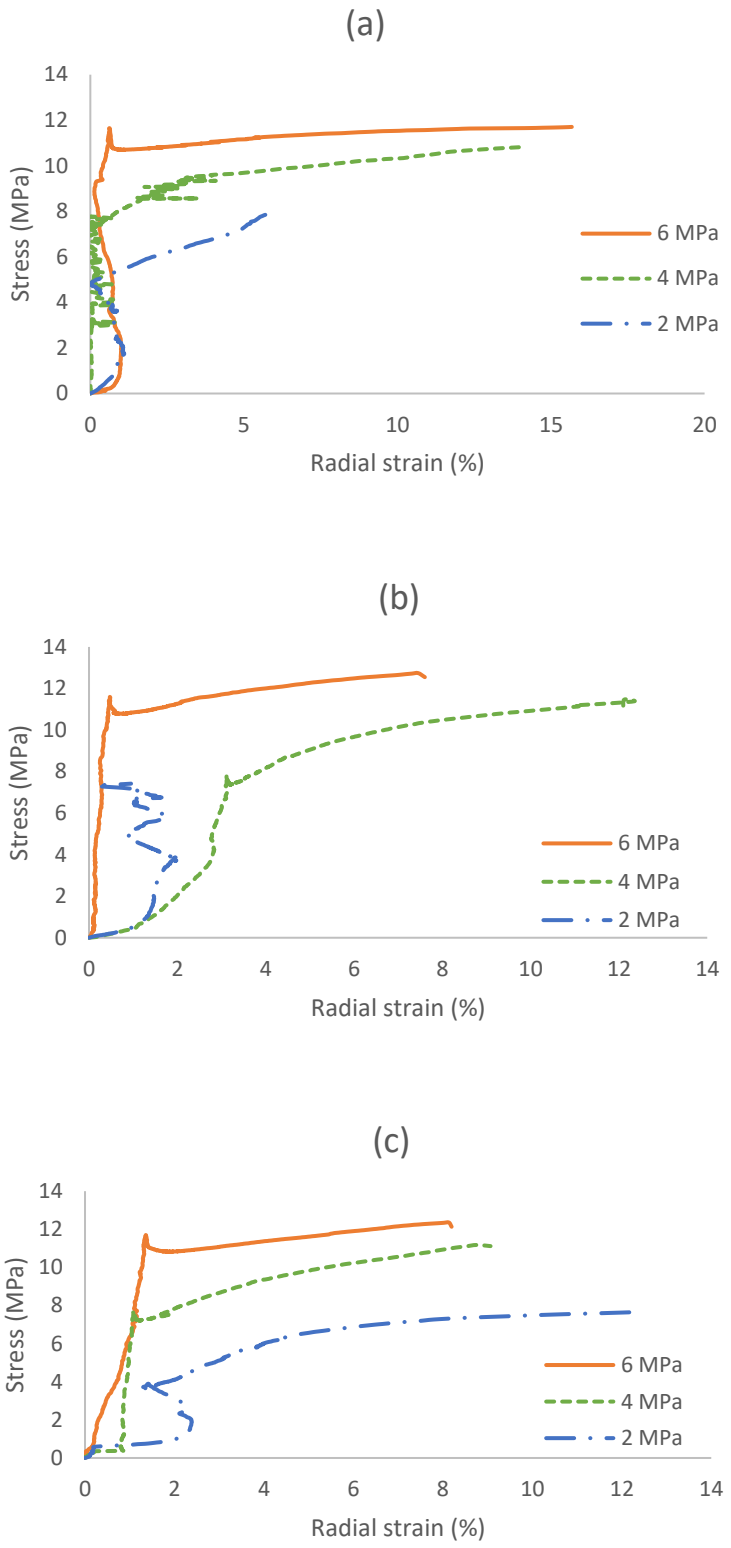


Fig 7. (a), (b) and (c) present the results on applying the third stress path on the TWHC specimens with 10%, 12% and 14% cement contents under 2MPa, 4MPa and 6MPa respectively.

The confining and vertical stresses were considered for an element at the borehole wall based on the lateral and axial stresses applied on the boundary of the TWHC specimens. The stresses were applied to the specimen at the same rate until a given value was reached. Then the confining stress was increased until an instability at the borehole wall was observed, while the vertical stress was kept unchanged. The main difference between the second and third stress paths was in the initial stage of the test, in which the axial stress applied to the specimen was considerably higher in the third path for the corresponding borehole size and specimen outer diameter. According to Fig 7 (a), with an increase in the vertical stress, the strength of the specimen reached prior to the initiation of the borehole failure was noticeably higher on the specimen with 14% cement under 6MPa than the specimen that was under 4MPa and 12% of cement content. It illustrates that the effect of vertical stress as a supporting pressure in increasing the ductility for a given cement content and the specimens exhibited a higher ductile behaviour when a greater vertical stress was applied. Furthermore, with increasing cement content, the borehole failure at the wall was observed at higher radial strains.

Unlike the specimens under the first stress path, the trends of graphs from the third stress path in general show that the vertical stress kept the specimen in the contraction mode and therefore, the dilation was observed at higher radial strains. The results also showed that with an increase in cement content, the radial strain would be increased for certain vertical stress in this stress path similar to that in the second stress path. This confirms that with an increase in the cement content, the lateral strain increases in all the stress paths. However, the effect of cement content had less influence than the change in vertical stress. Increasing cement content from 10% to 12% did not result in any significant variation in radial strain.

*3.4 Fourth Stress Path*

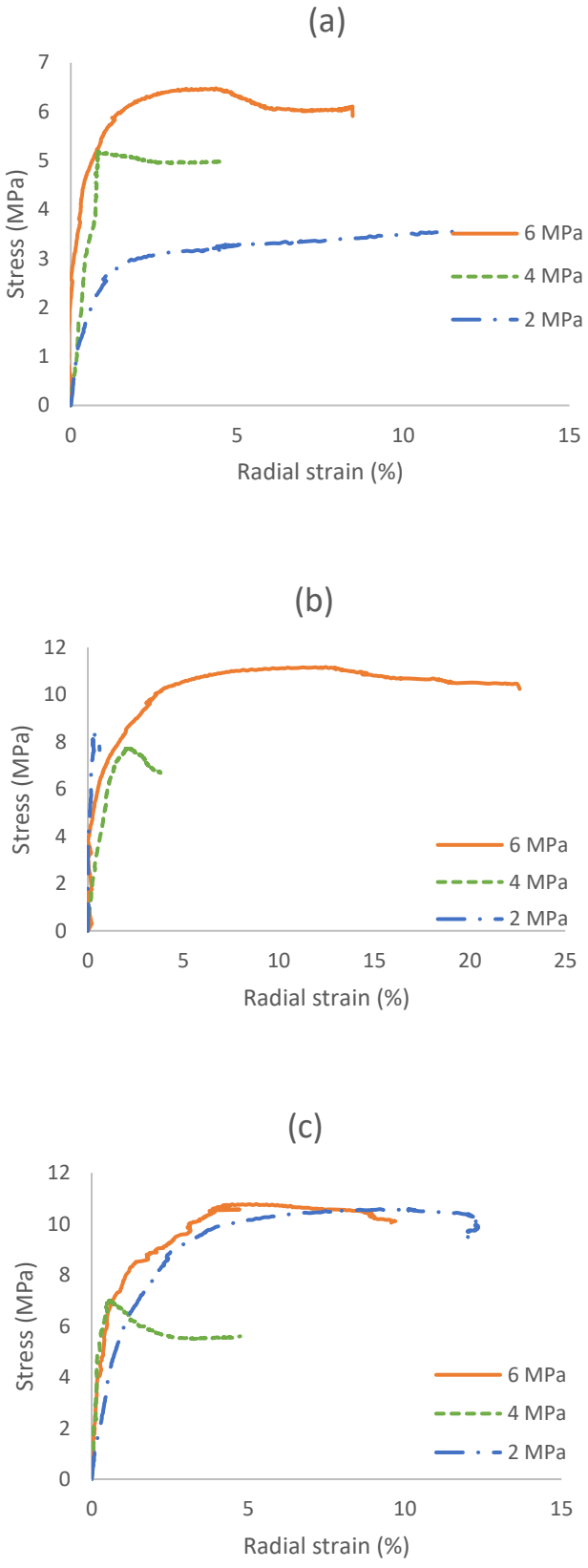


Fig 8: Deviatoric stress versus radial strain: (a) 10% cement content, (b) 12% cement content, (c) 14% cement content

Fig 8 (a), (b) and (c) illustrate the stress strain behaviour for the fourth stress path for 10%, 12% and 14% cement content respectively. In this path, the confining stress at the borehole wall was increased along with the axial stress at the same rate up to 2MPa. Then vertical stress was increased while confining stress was kept unchanged. The trend of the stress-strain relationships in the fourth path was similar to ones in the first path where the axial stress was much lower than that for the fourth path in the initial stage of the test. Fig 8 a-c show that the borehole instability occurs at a higher stress and lower radial strain for the fourth path in different cement contents. Since the initial axial stress was higher for the fourth path, the specimens behaved in a brittle manner before the borehole convergence. Such behaviour is likely to be due to the effect of the loading rate on the strength of the tested specimens.

*3.5 Fifth Stress Path*

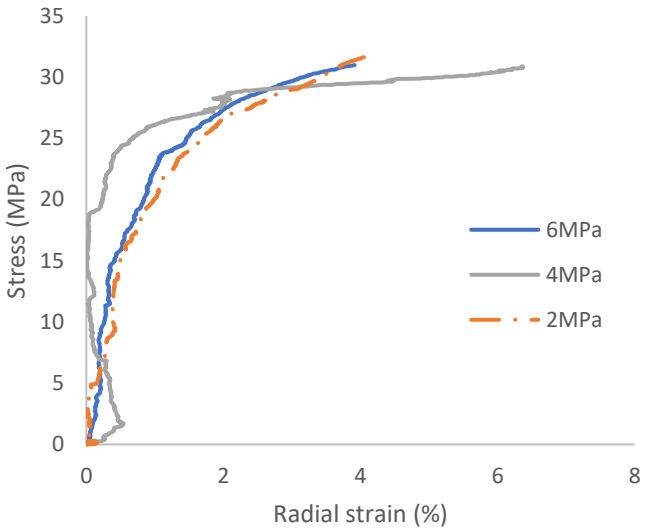


Fig 9: Deviatoric stress versus radial strain

In the fifth stress path, both σ$\theta$ and σr were increased simultaneously at the same rate until the failure at the borehole wall was observed by the camera. While the yield stresses increase consistently with the increase in the cement content, the specimens with 12% cement content behaved differently. For these specimens, the measured radial strain was significantly higher

at a lower stress state, compared to the specimens with 10% and 14% of cement content. This is likely to be caused by one of the two CMDs being placed at a location in the borehole where the borehole converged significantly more than at the other CMD. Therefore, the averaging of the two CMD readings resulted in such a different reading compared to the results obtained for the other cement contents. The yield stress for specimen with 10% cement content was significantly less than the specimen with 14% cement content. The TWHC specimens with 10% and 14% cement content behaved similarly as is indicated by the stress versus radial strain behaviour. When compared to that of the first and second stress paths where the confining pressure and axial stress were increased at a constant rate in the fifth stress path, the specimens tolerated a higher level of stresses surpassing 25 MPa as can be seen in Fig 9. It is important to mention that the trend of the graph remained unchanged for different levels of stresses applied, demonstrating the consistent contraction mode under the fifth stress path.

# 4. Conclusion

The effects of five different stress path regimes and three different cement agent contents on the borehole failure stress were investigated experimentally using the TWHC tests. Five different stress regimes were applied to the synthetic TWHC poorly cemented sand specimens with the CMDs deployed inside the borehole. In conjunction with the CMDs, the borehole was monitored by the camera. The five different stress paths included applying normal and strike-slip faulting stress regimes to synthetic TWHC poorly cemented sand specimens. The specimens under the first stress path showed that increase in the cement content in-creased the radial strain. The increase in the cement content had a minimal effect on the stiffness of the specimens tested under the second stress path. The specimens under third stress path showed that the radial strain increased with the increase in cement content. The effect of cement content had less influence on the borehole failure under the fourth stress path than the

change in vertical stress. The specimens under the fifth stress path tolerated a higher level of stresses. Finally, the effect of the cement content on the borehole failure was found to be more significant than the effect of confining pressure in all stress paths.

# 5. References


1. Amadei, B. and O. Stephansson . 1997. Rock Stress and Its Measurement. 1st ed. Chapman & Hall
2. Bujok, P., Porzer, M., Labus, K., Klempa, M. and Pavluš, J. (2013). Experimental modeling of abandoned shallow oil wells convergence. *Engineering Geology*, 157, pp.1-7.
3. Chen X, Wu S. (2013). Influence of water-to-cement ratio and curing period on pore structure of cement mortar. *Construction and Building Materials*; 38:804-812
4. Fjar, E., Holt, R., Raaen, A., Risnes, R. and Horsrud, P. (2008). *Petroleum related rock mechanics*. 2nd ed. Amsterdam: Elsevier, pp.309-310.
5. Galván V, Kanji MA. Simulation of arenaceous weak rocks by means of cemented sands. In: Proceedings of the 12th International Congress of International Society for Rock Mechanics. Beijing: CRC Press; 2011. pp. 751e2;
6. Goto, S., Tatsuoka, F., Shibuya, S., Kim, Y. and Sato, T. (1991). A simple gauge for local small strain measurements in the laboratory. *SOILS AND FOUNDATIONS*, 31(1), pp.169-180.
7. Haimson BC, Song I. Laboratory study of borehole breakouts in Cordova Cream: a case of shear failure mechanism. Int J Rock Mech Min Sci 1993; 30:1047–56.
8. Hashemi, S.S, Melkoumian, N., Taheri, A. and Jaksa, M. (2015). The failure behavior of poorly cemented sands at a borehole wall using laboratory tests. *International Journal of Rock Mechanics and Mining Sciences*, 77, pp.348-357.

9. Hashemi S.S and Melkoumian N. (2016) Effect of different stress path regimes on borehole instability in poorly cemented granular formations. *Journal of Petroleum Science and Engineering*. 146:pp.30-49
10. Igarashi. A., T. Ito, K. Sekine and K. Hayashi. 2008. Development of borehole tangential deformation gage and its application for determining the stress in rock. In Proceedings of the 42nd US Rock Mechanics Symposium and the 2 nd U.S. - Canada Rock Mechanics Symposium, San Francisco, 29 June – 2 July 2008 .
11. Li, J., Zhang, G. and Liu, M., 2019. Experimental investigation on the effect of confining pressure on the tensile strength of sandstone using hollow cylinder tensile test method. *Arabian Journal of Geosciences*, 12(24).
12. Liévano, V.R. and Kanji, M.A., 2011, October. Simulation of arenaceous weak rocks by means of cemented sands. In 12th ISRM Congress. OnePetro.
13. Papamichos E, Tronvoll J, Skjaerstein A, Unander TE (2010) Hole stability of red wildmoor sandstone under anisotropic stresses and sand production criterion. J Pet Sci Eng 72:78–92
14. Rawlings, C.G., Barton, N.R., Bandis, S.C., Addis, M.A. and Gutierrez, M.S., 1993. Laboratory and numerical discontinuum modeling of wellbore stability. Journal of Petroleum Technology, 45(11), pp.1086-1092.
15. Saidi, F., Bernabé, Y. & Reuschlé, T. 2003. The mechanical behaviour of synthetic, poorly consolidated granular rock under uniaxial compression. Tectonophysics, 370, 105-120.
16. Wu, B., Z. Chen and X. Zhang. Stability of borehole with Breakouts – An Experimental and Numerical Modelling Study. ARMA 16 -466 presented at the 50th US Rock Mechanics/Geomechanics Symposium, Houston, Texas. The USA .
17. Yan, M., Deng, J., Yu, B., Li, M., Zhang, B., Xiao, Q. and Tian, D., 2020. Comparative study on sanding characteristics between weakly consolidated

sandstones and unconsolidated sandstones. *Journal of Natural Gas Science and Engineering*, 76, p.103183.

18. Younessi A, Rasouli V, Wu B. Sand production simulation under true-triaxial stress conditions. Int J Rock Mech Min Sci 2013; 61:130–140.

# Chapter 3

# Study of Micro-parameters of DEM Model on the Laboratory Experiment Results Obtained from Poorly Cemented Sandstone

# (Journal Paper 3, Published)

Jun Hyuk Heo, Sam S. Hashemi and Noune Melkoumian

School of Civil, Environmental and Mining Engineering

The University of Adelaide, SA 5005, Australia

Publication:

Heo, J. H., Hashemi S.S. & Melkoumian, N. (2022). Study of Micro-parameters of DEM Model on the Laboratory Experiment Results Obtained from Poorly Cemented Sandstone. *Geosciences, 12(10), 373*

# Statement of Authorship

| | |
|---|---|
| Title of Paper | Study of Micro-parameters of DEM Model on the Laboratory Experiment Results Obtained from Poorly Cemented Sandstone |
| Publication Status | ☑ Published ☐ Accepted for Publication ☐ Submitted for Publication ☐ Unpublished and Unsubmitted work written in manuscript style |
| Publication Details | Heo, J. H., Hashemi S.S. & Melkoumian, N. (2022). Study of Micro-parameters of DEM Model on the Laboratory Experiment Results Obtained from Poorly Cemented Sandstone. Geosciences, 12(10), 373 |

## Principal Author

| | |
|---|---|
| Name of Principal Author (Candidate) | Jun Hyuk Heo |
| Contribution to the Paper | Performed numerical simulation, analysed data and wrote the manuscript. |
| Overall percentage (%) | 70% |
| Certification: | This paper reports on original research I conducted during the period of my Higher Degree by Research candidature and is not subject to any obligations or contractual agreements with a third party that would constrain its inclusion in this thesis. I am the primary author of this paper. |
| Signature | Date 13/11/2022 |

## Co-Author Contributions

By signing the Statement of Authorship, each author certifies that:

i. the candidate's stated contribution to the publication is accurate (as detailed above);

ii. permission is granted for the candidate in include the publication in the thesis; and

iii. the sum of all co-author contributions is equal to 100% less the candidate's stated contribution.

| | |
|---|---|
| Name of Co-Author | Dr. Sam S. Hashemi |
| Contribution to the Paper | Conceptulisation, supervision and review of the manuscript. |
| Signature | Date 11/14/2022 |

| | |
|---|---|
| Name of Co-Author | Dr. Noune Melkoumian |
| Contribution to the Paper | Supervision and review of the manuscript. |
| Signature | Date 21.11.2022 |

Please cut and paste additional co-author panels here as required.

# Abstract

Borehole convergence during or after drilling is one of the primary indicators of borehole instability. Early recognition of borehole instability is critical in achieving successful and timely completion of drilling operations and for borehole exploitation. A series of numerical simulations was conducted to investigate the borehole convergence of poorly cemented sandstones using Discrete Element Method (DEM). Rectangular 2-dimensional Particle Flow Code 2D (PFC2D) models were generated to study effect of contributing micro-parameters such as stiffness ratio, friction angle, friction coefficient and effective modulus on the behaviour of poorly cemented sandstone subjected to triaxial compression tests. A good agreement between the calibrated numerical models and the experimental data obtained from the laboratory was observed. The results showed that stiffness ratio was found to be a dominant factor in calibrating the numerical model, and the friction coefficient was the most influential micro-parameter.



Keywords: Borehole deformation; particle flow code; thick-walled hollow cylinder; poorly cemented sandstone


# 1. Introduction

Drilling exploration boreholes in the ground is one of the most widely used methods for investigating the subsurface formations in energy and mineral resources industry. As with any other excavation, drilling a borehole disturbs local pre-existing stresses in the vicinity of an opening, and this may result in rock failure due to the induced local stresses exceeding the rock strength. In practice, borehole instabilities may occur seemingly unpredictably at any stage of the drilling operations, resulting in the loss of time and equipment, as well as, in extreme cases, in abandoning the borehole (Fjar et al., 2008). It has been estimated that about

70 % of the world's hydrocarbon reservoirs are found within poorly cemented formations, where borehole instabilities are most likely to occur (Bianco and Halleck, 2001). Furthermore, a significant number of exploration boreholes being drilled through poorly cemented formations worldwide, and particularly in Australia, often result in technical difficulties such as stuck pipes (Hashemi et al., 2015).

Borehole instability problems typically account for 5-10 % of the total drilling costs and add up to the annual cost of hundreds of millions of dollars worldwide (Al-Ajmi and Zimmerman, 2006). Therefore, predicting the poorly cemented rock behaviour in the vicinity of excavation is essential for maintaining its stability and, consequently, for reducing the drilling costs. Numerical modelling provides the possibility of simulating a synthetic material consisting of an assembly of rigid grains that interact at contacts. Cundall (1971) proposed the Discrete Element Method (DEM) to simulate the microstructure features and mechanical properties of intact rocks. The Particle Flow Code (PFC) is the most widely used DEM code in geomechanics, the PFC model is capable of simulating both granular and bonded materials as well as an interface that can be inserted into the bonded materials. The PFC model simulates the movement of particles and their mechanical interaction at pair-wise contacts. Previous studies show that borehole convergence of granular materials is affected by many factors, including the stress level, loading path, particle strength, degree of cementation and borehole size (Hashemi and Melkoumian, 2016). Among all these factors, the effect of degree of cementation has not been fully clarified. Limited study showed that stress level is dependent on the degree of cementation. However, the mechanism of the effect of degree of cementation on borehole convergence is still not clear. This may be due to the difficulties of carrying out experimental research on poorly cemented sandstone specimen. Numerical modelling enables investigation of how microscopic parameters of DEM model impact on the behaviour of the numerical model. The DEM provides an opportunity to incorporate the

damage mechanisms into force-displacement law of the contact which allows more realistic numerical framework compared to other numerical modelling methods. PFC has been used to simulate rock behaviour (Potyondy 2015). Recently, numerical models have been applied to simulate the progression of breakouts (Papanastasiou and Vardoulakis 1992; Rahmati et al. 2014; Duan and Kwok 2016; Lee et al. 2016; Setiawan and Zimmerman 2018; Li et al. 2019). This study focuses on the effect of contributing parameters such as stiffness ratio, friction angle, friction coefficient and effective modulus on the behaviour of poorly cemented sandstone subjected to triaxial compression tests using DEM. A comparison between experimental and numerical results was conducted to validate the outcome of the DEM simulations.

# 2. Discrete Element Modelling

*2.1 Bonded-particle model*

In the discrete element model, the boundary conditions do not only constrain the particle's motion, but also allow loading the specimen by setting its boundary's motion speed. There are three possible boundary conditions that can be configured in the PFC2D discrete element software: wall boundary; discrete particle boundary, and mixed boundary. The wall boundary was used in this study, and the loading fixture for the boundary wall simulation in the actual test was established on the upper and lower parts of the specimen, and a constant motion speed was applied to the wall element to simulate the loading speed during the actual test. Bonded Particle Model (BPM) can be utilised to numerically model and simulate the behaviour of both the mechanical and microstructural behaviours of intact rock particle assemblies bonded by cementations. The mechanical behaviours investigated in the literature include elasticity (Potyondy and Cundall 2004; Schöpfer et al. 2007), fracturing (Zhao et al. 2015; Zhou et al. 2016), failure processes (Duan et al. 2015b), damage zones (Fakhimi and Villegas 2007), rock cutting (He and Xu 2015), crack initiation and coalescence processes

(Vesga et al. 2008; Ning et al. 2015; Tian and Yang 2017) and shearing behaviours of soil-rock mixture (Xu et al. 2015).

PFC2D allows three BPMs, the linear-bonded model (LBM), the parallel-bonded model (PBM) and the flat-jointed model (FJM). The PBM and FJM are the most widely used in rock simulations, which enables simulating an excellent match of mechanical behaviours of rocks at lab scales. However, a BPM with a LBM or a PBM suffers from three intrinsic problems: unrealistic ratio of uniaxial compressive strength (UCS) to tensile strength (TS), unrealistic low internal friction angle, and unrealistic linear failure envelope (Potyondy and Cundall 2004; Cho et al. 2007; Schöpfer et al. 2007; Wu and Xu 2016). These limitations can be addressed in two ways: By either increasing interlock in the numerical models, i.e. creating clumps of particles (Cho et al. 2007), which increases computation time; or by introducing a grain-based model. The calculations performed in the DEM alternate between the application of Newton's second law to the particles and a force-displacement law at the contacts. Newton's second law is used to determine the motion of each particle arising from the contact and body forces acting upon it, while the force-displacement law is used to update the contact forces arising from the relative motion at each contact. One of the major issues identified using BPM is the bond failure and contact stress reduction leading to an abrupt energy release in DEM simulation. a gradual yielding of the bonds is involved in the process of fracture initiation and propagation (Khazaei et al. 2015). In order to make the bond breakage process in DEM more realistic, a softening constitutive model can be assigned on the DEM contacts. Such softening response at microscopic level allows controlling of the overall energy dissipation of the simulation while maintaining stable macroscopic failure growth.

### *2.2 Constitutive relationships*

In DEM simulation, macroscopic failure behaviour is controlled by the contact constitutive models. Hence, the failure characteristics of the material, i.e. gradual softening, must be

appropriately incorporated in the contact model. There are several cohesive models available in the literature (Le et al. 2017, 2018; Nguyen et al. 2017a; Nguyen et al. 2017b) that can be used as contact models in DEM.

*2.3 Calibration*

The micro-parameters must be calibrated prior to comparing the results of the DEM with the laboratory experimental results. The selection of an appropriate set of micro-parameters is a critical step in DEM simulation. The most commonly used method of calibrating the micro-parameters of PFC DEM includes comparing the results of uniaxial compressive tests and triaxial tests of a physical specimen obtained from the laboratory and reproduce the macroscopic behaviour of the physical specimen (Bahaaddini et al. 2013; Gutiérrez-Ch et al. 2018). In this study, a series of laboratory experimental test results obtained from synthetic poorly cemented sandstone specimens were used. The micro parameters of the numerical model were calibrated against the laboratory experimental test results. The numerical macroscopic shear stiffness, normal stiffness, and friction coefficient were compared with their experimental counterparts.

The dimension of a physical specimen used for uniaxial compressive tests was 127 mm in height and 63.5 mm in width. A rectangular specimen matching the physical specimen dimension was created in PFC2D. The minimum particle radius ($rmin$) was chosen to be 0.225 mm, and the ratio of the maximum particle radius ($rmax$) to minimum particle radius ($rmin$) was chosen to be 1.66 as it is the most common choice for the simulation of rocks (Koyama and Jing 2007). The inverse calibration method was used to obtain the micro parameters such as the contact strength, the softening parameter, the friction of coefficient, normal to shear stiffness ratio, dilation coefficient of the cohesive contacts.

The contact deformability method proposed by Potyondy and Cundall (2004) was employed to calibrate the model. The first step involved matching the macroscopic Young's modulus with its experimental counterpart. The linear elastic behaviour of the DEM specimen is controlled by Effective modulus and the friction of coefficient. These two parameters were modified to match the macroscopic Young's modulus. During the calibration of the linear elastic stage, the contact strength was considered to be high enough to avoid any possible damage in the specimen. The subsequent step is to calibrate the Poisson's ratio ($\upsilon$) which is controlled by normal to shear stiffness ratio. This parameter was calibrated in an iterative procedure with the first stage of calibration. Finally, the UCS of the model was reproduced by altering the bonding parameters, the friction coefficient of the contacts, and the softening parameter. The strength of the cohesive contacts was controlled by the bonding parameters, and the softening parameter controls the softening behaviour of the contacts during post-peak stage. The friction coefficient of the contacts also influences the strength of the contacts, which in the macroscopic scale can control the UCS of the model.

In the model generation stage, the rectangular boundary wall was established in PFC2D. the wall uses the software's built-in FISH language to achieve particle delivery. In the process of generating the target porosity using the shrink-and-expansion method, the wall stiffness needs to be set to prevent particles from escaping from the model boundary. The solid model and hollow cylinder model generated in PFC2D are shown below in Figure 1(a) and Figure 1(b) respectively.

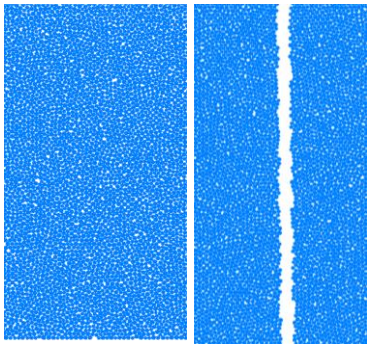

Figure 1: (a) Solid model generated in PFC, (b) Hollow cylinder model generated in PFC

Default procedure to set up PFC2D model for numerical simulations involved following the four steps below proposed by Potyondy and Cundall (2004).

1. Generate particles randomly with diameters in a specified range within a vessel bounded by frictionless walls
2. Adjust the system by allowing particles to move under zero friction
3. Apply a low isotropic stress by modifying the diameters of all particles simultaneously
4. Modify the diameters of particles that have less than two contacts iteratively so that these particles have at least two contacts.

The numerical model used for the calibration is a cylinder with a diameter of 63.5 mm and a height of 127 mm and was generated using the default procedure listed above in PFC2D. After a numerical model is generated, the specimen is confined by top, bottom and side walls. The specimen is loaded by moving the top and bottom walls toward each other at a specified loading rate that ensures a quasi-static loading condition. A constant loading at a displacement rate of 0.07 mm/min was applied to keep the numerical simulation results comparable to experimental laboratory test results. Simulation time was largely dependent on the minimum radius size of the ball particles where a specimen with the minimum ball radius of 0.25 mm as shown in Figure 1 (a) took approximately 13 minutes to simulate.

Figure 2 illustrates a comparison of stress-strain curves obtained from DEM and laboratory tests under 2MPa of confining pressure for solid specimens. A close agreement was observed between the experimental data and the calibrated numerical results.

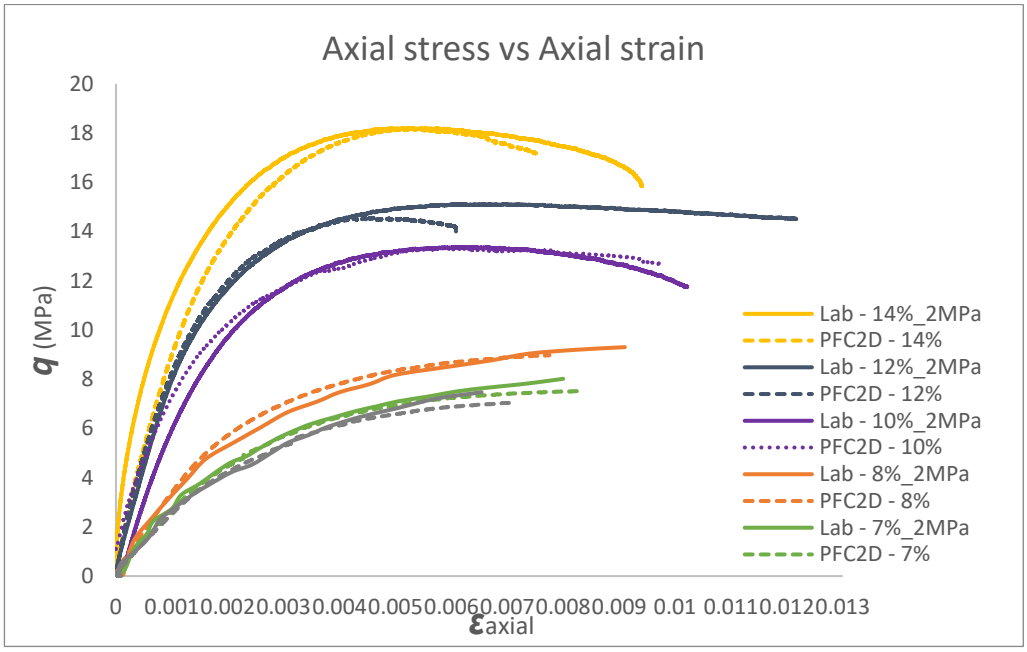


Figure 2. Comparison of the triaxial test results from the laboratory experiment and DEM simulations

# **3.** Experimental Test Results

The synthetic sandstone specimens used in this study were prepared according to the mixture preparation procedure for a poorly cemented formation proposed by Hashemi et al. (2015). The mixture was composed of natural silica sands with two different grain size ranges, namely, coarse grain sands with a grain size between 0.425 mm-1.4 mm, and fine grain sands with a grain size between 0.15 mm-0.355 mm, Portland cement type II (specific gravity, *Gs* = 3.15 *g/cm³*) and water. The components were thoroughly mixed together to achieve a homogeneous mixture for specimens, and the time spent between pouring water into the dry mixture and compacting it into metal moulds was maintained to be within 30 minutes to avoid initial setting of the cement. Each sample was prepared by compacting the mixture into three equal layers of 42 mm thickness. The top surface of the bottom layer was scratched before

the subsequent layer was compacted on top of it to ensure thorough interlocking between the successive layers. The mixture was not strong enough to bond sand grains in the early curing stage. Thus, the samples were left in the mould for five days, and then were removed from the mould and cured for another three days wrapped in a plastic film at room temperature (18-23°C) before testing. Mechanical properties of the specimens are presented in Table 1.

Table 1 Mechanical properties of the synthetic specimens

| Cement content (%) | Uniaxial Compressive Strength (MPa) | Poisson's ratio (ν) | Bulk density $\rho$ $(\frac{kg}{m^3})$ |
|---|---|---|---|
| 10 | 4.96 | 0.243 | 1792 |
| 12 | 7.34 | 0.237 | 1859 |
| 14 | 9.90 | 0.231 | 1913 |

Figure 3 below shows the picture of synthetic cylinder and TWHC specimens used for laboratory testing.

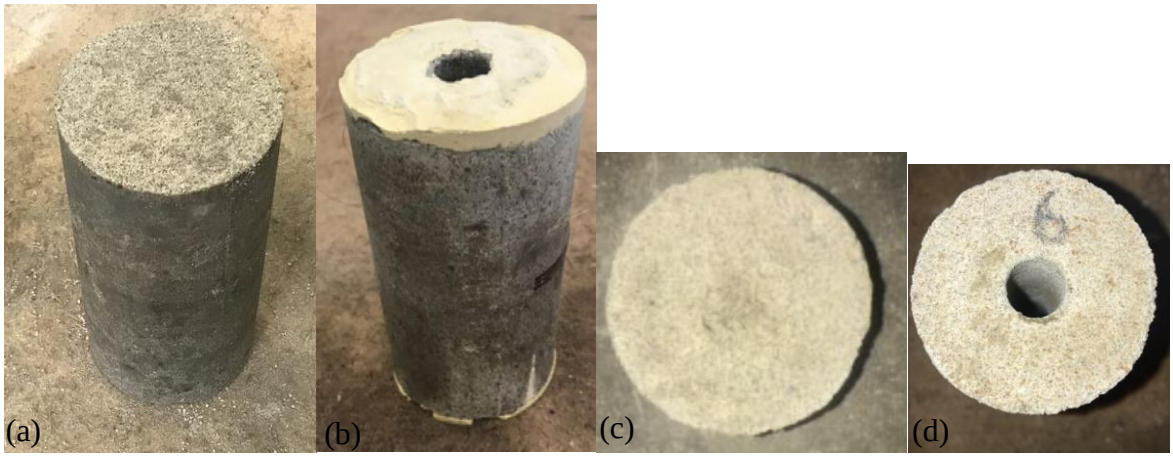


Figure 3. (a) Cylinder sample side view, (b) TWHC sample side view, (c) Cylinder sample top view (d) TWHC sample top view

UCS tests were conducted on cylinder specimens. The UCS test results showed that the maximum strength and the pre-maximum stiffness increase as the cement content was increased. The influence of cement content on the peak strength was substantial. The UCS increased by 48% when the cement content was increased from 10 % to 12 %. Further increases in the cement content to 14 % and 16 % resulted in 35 % and 25 % increase in the UCS respectively, indicating that the influence of the cement content on the maximum

strength becomes less significant as the cement content increases. This can be caused by the reduction in the grain to grain space available for cementation due to the increased cement content which pushes grains closer. Furthermore, according to Chen and Wu (2013), low water to cement ratio results in decreased cement hydration. Thus, the increase in the cement content for the same water content could also have contributed to the reduced cement hydration due to excess cement particles not reacting with water. Laboratory studies by Saidi et al. (2003) also observed that in granular materials adding an additional cementing agent to the specimens with a low cement content of less than 20 % is more likely to significantly increase their maximum strength, than adding a more cementing agent to the specimens with a higher cement content. The post-peak stress-strain trend of samples with 10 % cement content showed a greater ductile behaviour compared to the samples with a higher cement content of 12 % and 14 %. Moreover, the effect of water content was studied by varying the amount of water content between 10 % and 12 % while keeping other components unchanged. The increase in the water content resulted in strength reduction as a result of the increased total porosity. This outcome is in agreement with previous studies by Hashemi et al. (2015) conducted on synthetic sandstones with 10 % water content.

### *3.1 Cut-off UCS*

Poorly cemented sandstones are characterized by low strength, poor cementation and high porosity (Bosio and Kanji, 1998). The UCS test results are generally considered for classification of weak sandstones from stronger hard rocks (ISRM 1981, He 2014 and Kanji 2014). In this study, Baud and Gambin (2011)'s approach for selecting the soft rocks based on the UCS upper limit of 10 MPa, as well as Liu and Wu (2016)'s guidance on classifying weak sandstone from stronger sandstone based on the UCS have been taken into consideration. To identify the mechanical properties a series of UCS tests were conducted on synthetic sandstones with various cement contents while keeping the water and sand components

constant. Synthetic sandstone samples with four different cement contents, namely 10 %, 12 %, 14 %, and 16 % were considered for studying the effect of cement content on the UCS. These UCS tests were conducted based on the ISRM suggested methods (ISRM 1981) and under the same testing conditions.

Figure 4 a-c illustrate the compactor used to achieve uniform compaction of the specimen mixture in the mold, the synthetic rock specimens cast in the metal molds, and the final solid synthetic specimens prepared for UCS testing respectively. The specimens were tested after 8 days of curing time and the average dry density was measured to be 1.79 g/cm$^3$.

Figure 4. (a) Compactor, (b) Samples in the molds, (c) Unmoulded samples

The stress-strain diagrams obtained from the UCS tests are presented in Figure 5. The results showed that the maximum strength, $\sigma_{max}$ and the pre-maximum stiffness increase as the cement content increases. This trend is in agreement with the UCS test results obtained by Hashemi et al. (2015) who used a lower range of cement content between 5 % and 8 %. It was observed that an increase in the cement content resulted in a higher maximum strength which also matches closely with other studies conducted on the influence of cement content on the UCS of synthetic sandstone specimens (Bernabe et al. 1992 and Saidi et al. 2003).

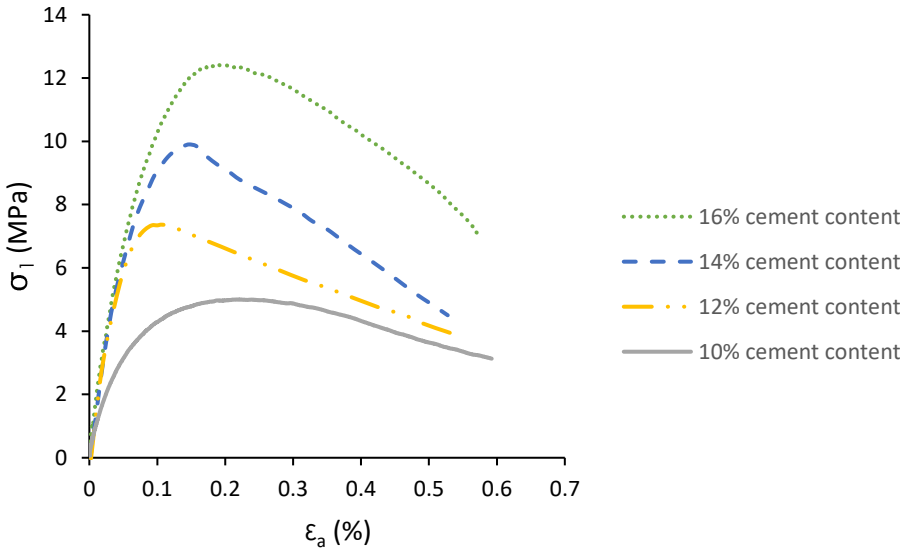


Figure 5. Stress versus axial strain behaviour for specimens subjected to UCS testing

As can be seen from Figure 5, the solid specimens with higher than 14 % cement content exceeded the UCS of 10 MPa, therefore, 14% was identified as the upper cut-off cement content for this study, as increasing the cement content beyond this level resulted in a stronger specimen which does not meet the strength characteristic of a poorly cemented rock (Klein 2001). Three cementation levels (i.e. 10 %, 12 % and 14 %) were considered for TWHC experiments.

*3.2 Triaxial test results on solid specimens*

Triaxial tests were carried out on solid cylindrical specimens with three different cement contents based on the preliminary UCS test results. Specimens with cement contents of 10 %, 12 %, and 14 % were tested under different stress conditions. Figure 6 a-c present the deviatoric stress ($\sigma_{deviatoric} = \sigma_1 - \sigma_{hydrostatic}$) versus the axial strain diagram for solid specimens with different cement contents.

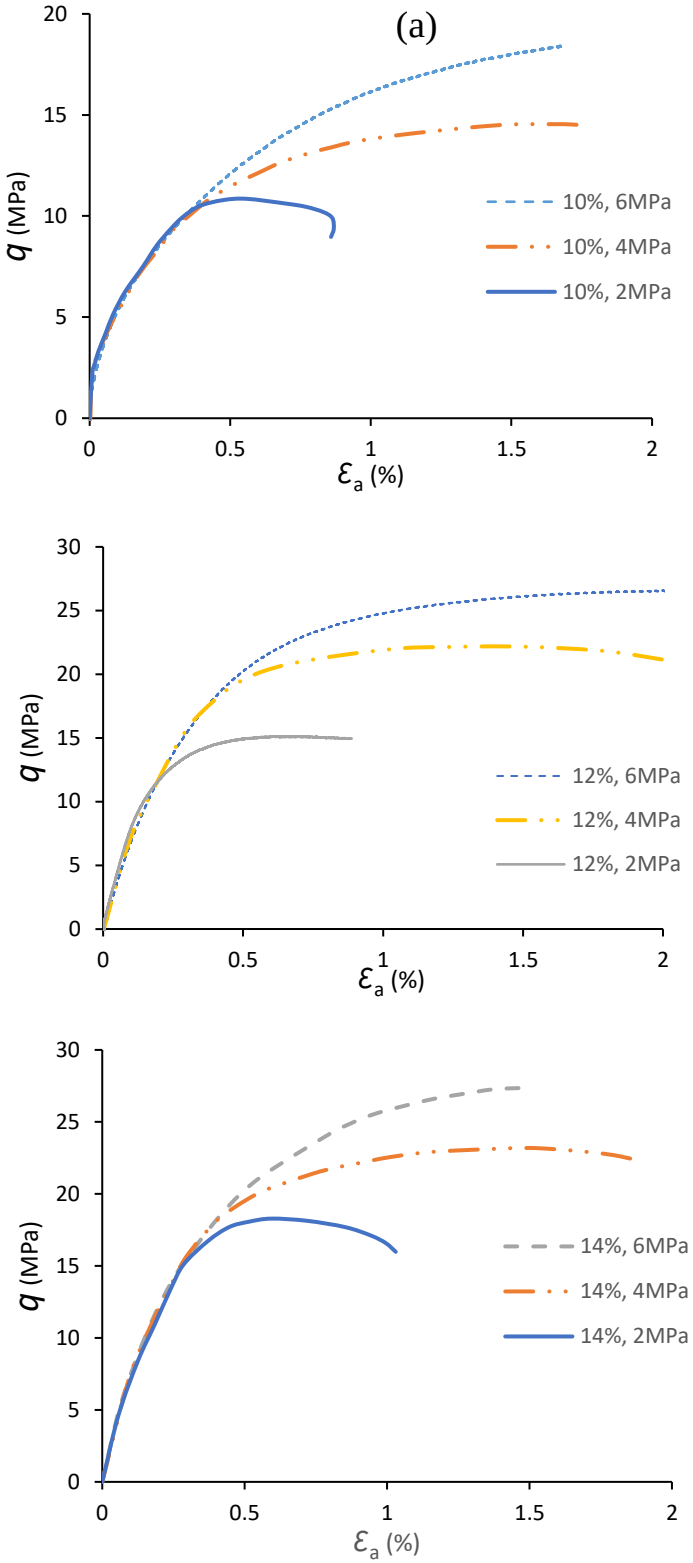


Figure 6. Deviatoric stress versus axial strain behaviour of solid specimens subjected to triaxial testing, (a) 10 % cement content, (b) 12 % cement content, (c) 14 % cement content

*3.3 Triaxial tests on thick-walled hollow cylinder specimens*

Triaxial tests were conducted on TWHC specimens with 15 mm diameter borehole for three different cement contents (10 %, 12 %, and 14 %) and various confining pressures. Figure 7

presents the deviatoric stress ($\sigma_{deviatoric} = \sigma_1 - \sigma_{hydrostatic}$) versus the axial strain diagram for TWHC specimens with cement contents between 10% and 14%.

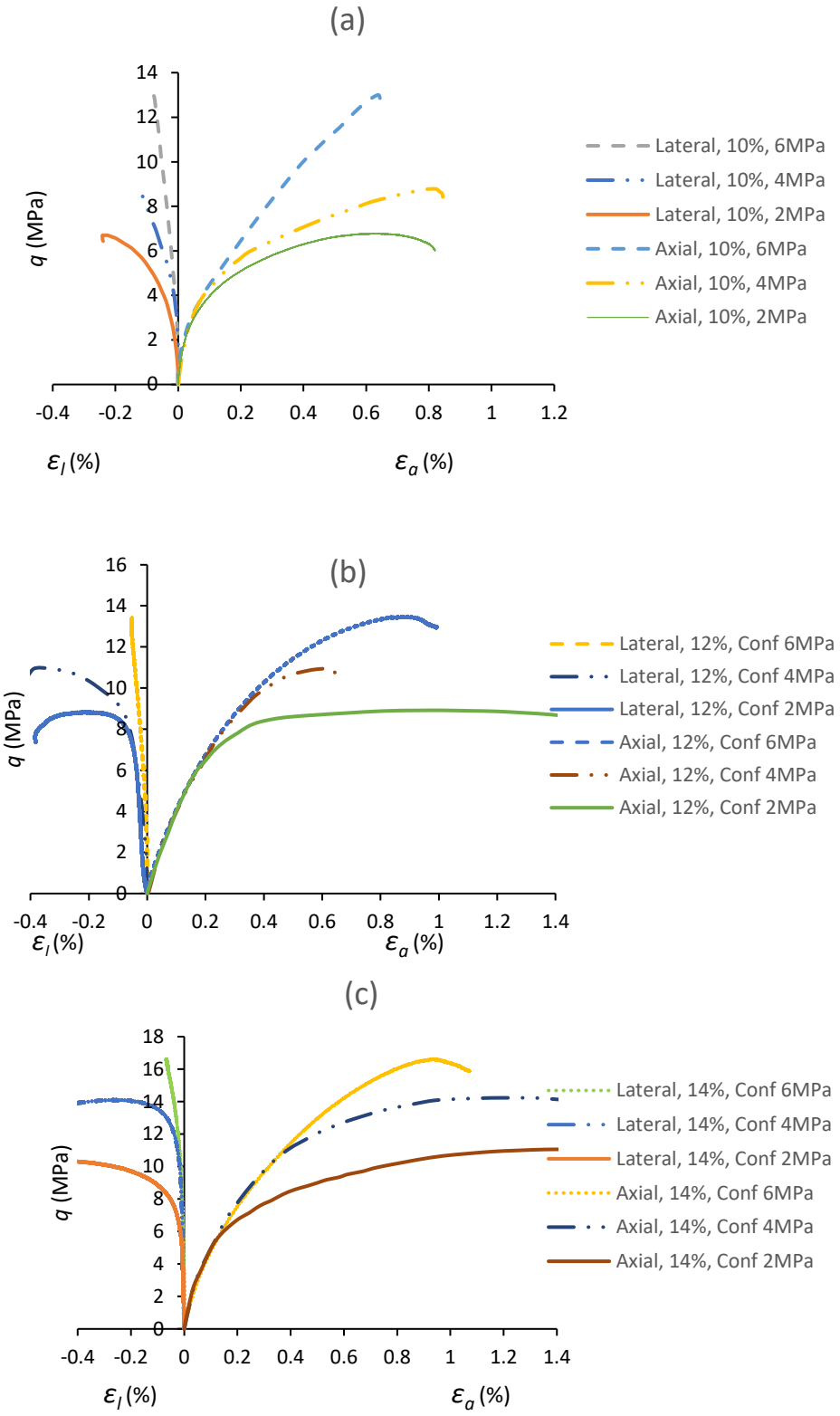


Figure 7. Deviatoric stress versus axial strain for TWHC specimens: (a) 10 % cement content, (b) 12 % cement content, (c) 14 % cement content

# 4. Numerical Simulation Results

*4.1 Stiffness ratio*

The effects of Stiffness ratio on the deviatoric stress q of the synthetic rock are illustrated in Figure 8 when Stiffness ratio increases from 0.5 to 1.5, the q of the numerical model increases along with the Young's modulus. These results are consistent with previous numerical simulation conducted by Huang (1999), Yang et al. (2006), Fakhimi and Villegas (2007) and He and Xu (2015) where Stiffness ratio is a dominant factor in calibrating the deviatoric stress q and Young's modulus E.

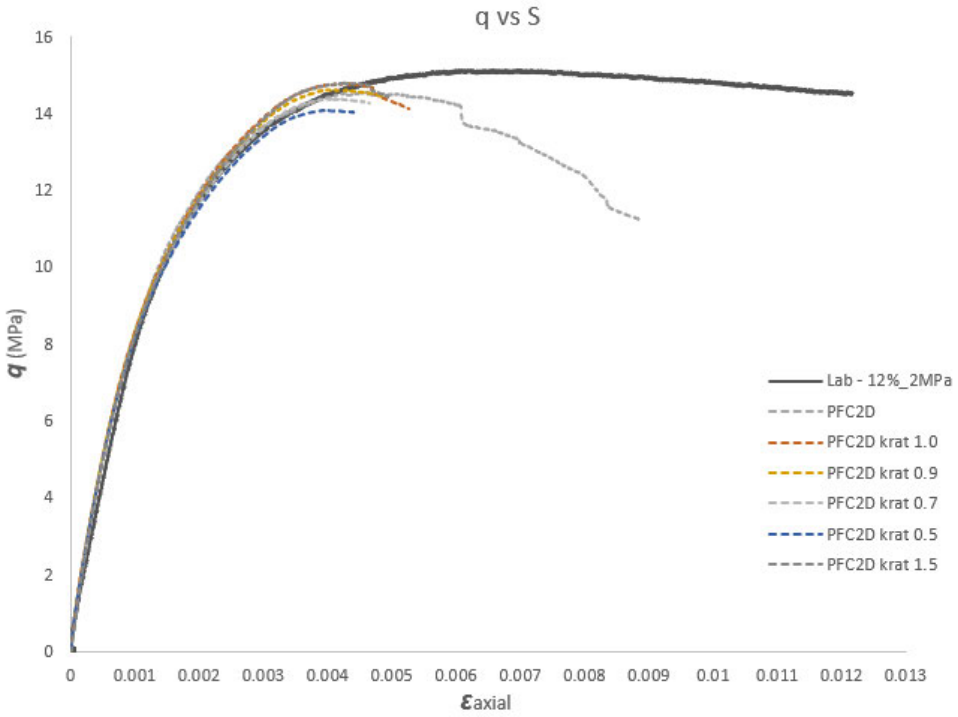


Figure 8. Variations in stiffness ratio on deviatoric stress q

*4.2 Friction angle*

Friction angle was varied to assess its influence on the deviatoric stress. The friction angle was varied between 10 degrees and 50 degrees as illustrated in Figure Figure 9. The variations in the friction angle below 40 degrees had limited impact on the deviatoric stress. The Friction angle has no influence on the Young's modulus until the friction angle increases above 40 degrees and this was due to the friction angle having no effect until the bond breaks and

sliding between particles occur. This observation is in agreement with Wu and Xu (2016)'s DEM numerical simulation results that showed the friction angle has no effect on the pre-failure macroscopic parameters.

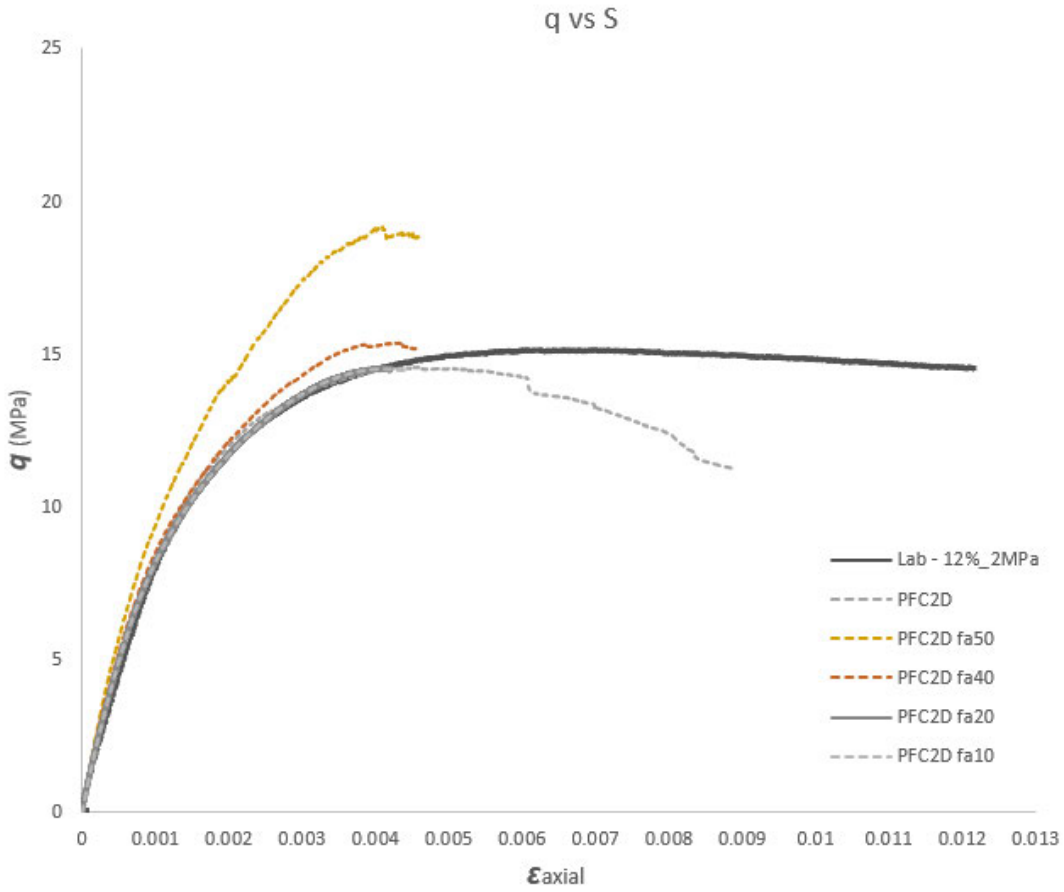


Figure 9. The effect of friction angle on deviatoric stress q

*4.3 Friction coefficient*

Figure 10 illustrates that the deviatoric stress increases with an increase in friction coefficient. This observation indicates that particle breakage of granular materials depends on the friction coefficient. The particle friction coefficient was the most influential micro parameter. When the friction coefficient was varied from 0.15 to 0.45, the deviatoric stress increased by threefold from 5 MPa to 15 MPa. Friction forces dominate the contact forces between particles during compression and as a result an increase in the friction coefficient resulted in an increase of the deviatoric stress. The PFC2D simulation of triaxial tests carried out by

Zhao et al. (2015) also demonstrated the significance of the particle friction coefficient. The simulation showed that particles with higher friction coefficient resulted in higher shear strength under compression which matches with this study. This may imply that there was quite a bit sliding movement between particles during compression, where friction between particles played a major role in the resultant shear strengths.

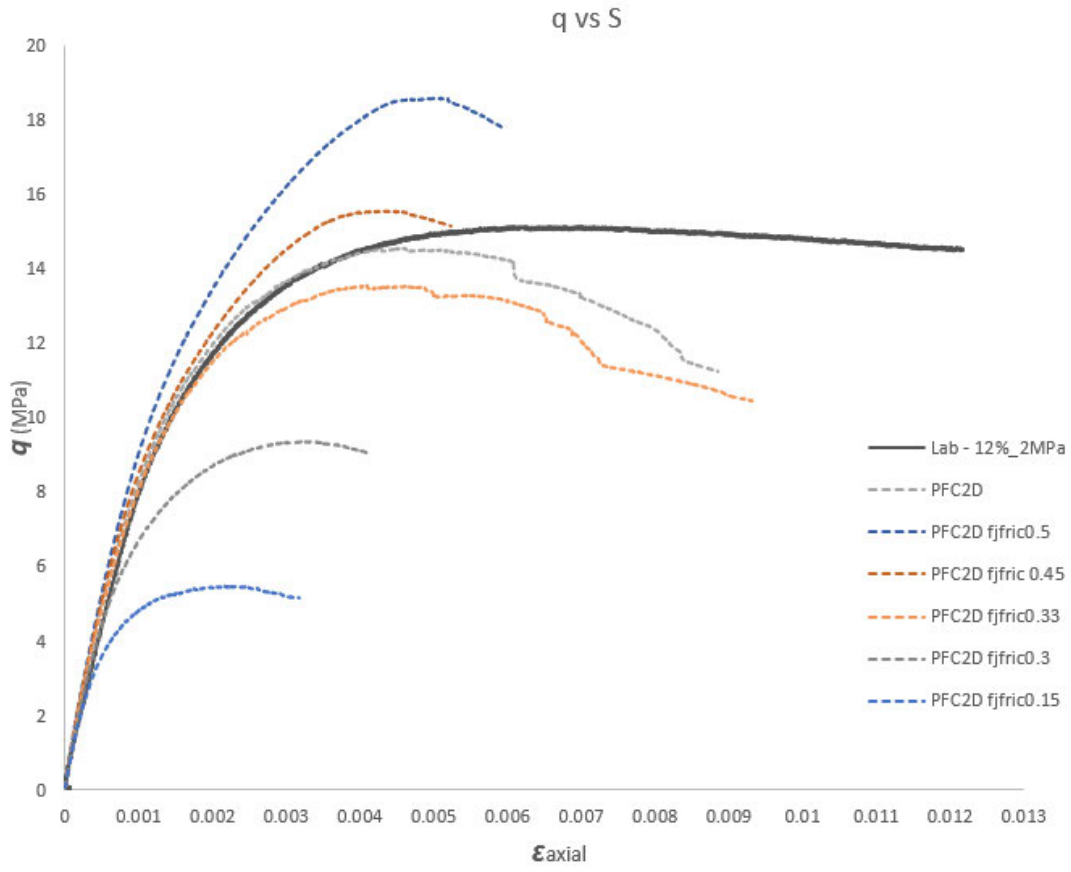


Figure 10. The effects of friction coefficient values on deviatoric stress q

*4.4 Effective modulus (E*)*

The effects of effective modulus values on the deviatoric stress are illustrated in Figure 10. An increase in the effective modulus resulted in an increase in both Young's modulus and the deviatoric stress. This result is consistent with a previous study completed by Zhou et al. (2018) where the Young's modulus E was found to be linearly dependent on the effective modulus. Furthermore, the effect of increasing the effective modulus values on the deviatoric stress compared to other micro-parameters was found to be greater.

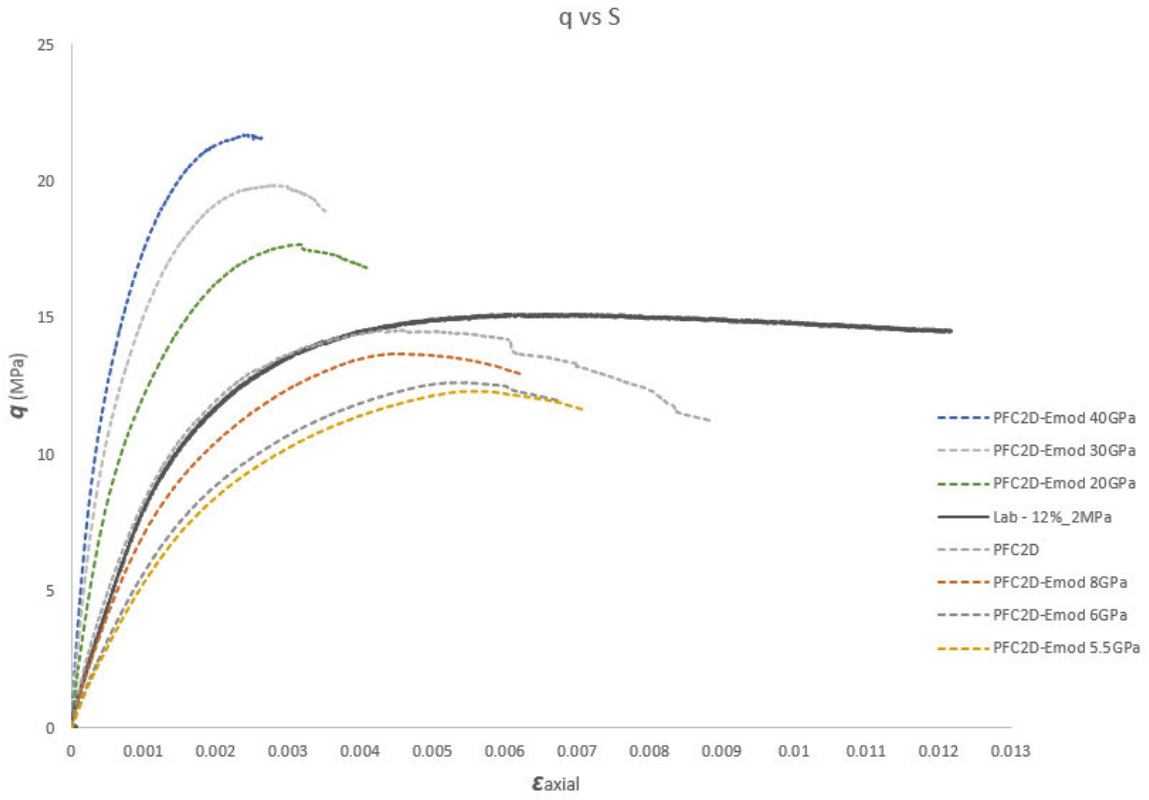


Figure 11. The effects of effective modulus values on deviatoric stress q

# 5. Conclusions

In conclusion, the PFC2D numerical models calibrated using the triaxial experimental data obtained from the laboratory showed good agreement in the deviatoric stress versus radial strain relationship in their experimental counterparts. Through various attempts of numerical simulations, the calibrated numerical models successfully simulated the behaviour of poorly cemented sandstone specimens tested in the laboratory.

The effects of micro-parameters such as stiffness ratio, friction angle, friction coefficient, and effective modulus were investigated to identify how each of the selected micro-parameters impacted the deviatoric stress under the triaxial test. The results showed that the particle friction coefficient is the most influential micro-parameter.

The presented numerical simulations using PFC2D have helped to gain a better understanding of the effects of various micro-parameters on the borehole deformation behaviour and failure stress. It is important to be able to predict the behaviour of poorly cemented sandstone to understand the detailed failure propagation developed under different confining pressures.

# 6. References


1. Al-Ajmi, A. and Zimmerman, R. (2006). Stability analysis of vertical boreholes using the Mogi–Coulomb failure criterion. International Journal of Rock Mechanics and Mining Sciences, 43(8), pp.1200-1211.

2. Bahaaddini, M., Sharrock, G., & Hebblewhite, B. K. (2013). Numerical direct shear tests to model the shear behaviour of rock 416 joints. Computers and Geotechnics, 51, 101-115.

3. Baud JP, Gambin M. Classification of soils and rocks based on pressuremeter tests under high pressure. In: Proceedings of the 15th European Conference on Soil Mechanics and Geotechnical Engineering. Athens: Mill Press; 2011. pp. 325e30.

4. Bernabe, Y., Fryer D, & Hayes J. (1992) The effect of cement on the strength of granular rocks. *Geophys Res Lett*; 19:1511-1514.

5. Bosio JJ, Kanji MA. Soft rocks of the Rio de la Plata Basin. In: International Symposium on Indurated Soils and Soft Rocks, AGI, Naples. Rotterdam: A.A. Balkema;1998. pp. 65e71.

6. Bianco, P.M., and Halleck. (2001), Mechanisms of arch instability and sand production in two-phase saturated poorly consolidated sandstones, in SPE European Formation Damage Conference, the Hague, Netherlands

7. Chen X, Wu S. (2013). Influence of water-to-cement ratio and curing period on pore structure of cement mortar. *Construction and Building Materials*; 38:804-812

8. Cho, N. A., Martin, C. D., & Sego, D. C. (2007). A clumped particle model for rock. International journal of rock mechanics and 402 mining sciences, 44(7), 997-1010.

9. Duan, K., Kwok, C. Y., & Pierce, M. (2016). Discrete element method modeling of inherently anisotropic rocks under uniaxial 388 compression loading. International Journal for Numerical and Analytical Methods in Geomechanics, 40(8), 1150-1183.

10. Fjar, E., Holt, R., Raaen, A., Risnes, R. and Horsrud, P. (2008). *Petroleum related rock*

*mechanics*. 2nd ed. Amsterdam: Elsevier, pp.309-310.

11. Gutiérrez-Ch JG, Senent S, Melentijevic S, Jimenez R. (2018) Distinct element method simulations of rock-concrete interfaces under different boundary conditions. Engineering Geology 240: 123-139.

12. Fakhimi A, Villegas T (2007) Application of dimensional analysis in calibration of a discrete element model for rock deformation and fracture. Rock Mech Rock Eng 40:193–211.

13. Hashemi, S.S, Melkoumian, N., Taheri, A. and Jaksa, M. (2015). The failure behavior of poorly cemented sands at a borehole wall using laboratory tests. *International Journal of Rock Mechanics and Mining Sciences*, 77, pp.348-357.

14. Hashemi S.S and Melkoumian N. (2016) Effect of different stress path regimes on borehole instability in poorly cemented granular formations. *Journal of Petroleum Science and Engineering*. 146:pp.30-49

15. He X and Xu C (2015). Discrete element modelling of rock cutting: from ductile to brittle transition. Int J Numer Anal Methods Geomech 39:1331–1351.

16. Huang H (1999) Discrete element modeling of tool-rock interaction (Doctoral dissertation). The University of Minnesota.

17. ISRM. (1981), Rock characterization, testing, and monitoring. ISRM suggested methods. International Journal of Rock Mechanics and Mining Sciences & Geomechanics Abstracts, 18(6), p.109.

18. Kanji, M. (2014). Critical issues in soft rocks. *Journal of Rock Mechanics and Geotechnical Engineering*, 6(3), pp.186-195.

19. Koyama T, Jing L (2007) Effects of model scale and particle size on micro-mechanical properties and failure processes of rocks-A particle mechanics approach. Eng Anal Bound Elem 31:458–472.

20. Khazaei C, Hazzard J, Chalaturnyk R. (2015) Damage quantification of intact rocks using acoustic emission energies recorded during uniaxial compression test and discrete element modeling. Computers and Geotechnics 67: 94-102.

21. Klein (2001). 'An approach to the classification of weak rock for tunnel projects' in Proceedings Rapid Excavation and Tunneling Conference. San Diego.

22. Le LA, Nguyen GD, Bui HH, Sheikh AH, Kotousov A, Khanna A. (2017) Modelling jointed rock mass as a continuum with an embedded cohesive-frictional model. Engineering Geology 228

23. Le LA, Nguyen GD, Bui HH, Sheikh AH, Kotousov A, Khanna A. (2018) Localised

failure mechanism as the basis for constitutive modelling of geomaterials. International Journal of Engineering Science accepted & in press.

24. Li, X., El Mohtar, C. S., & Gray, K. E. (2019). Modeling progressive breakouts in deviated wellbores. Journal of Petroleum Science 377 and Engineering, 175, 905-918.

25. Liu, K. and Wu, B. (2016). Predicting Reservoir Rock Mechanical Properties Directly from Sedimentary Characterisation. In: *SPE Asia Pacific Oil & Gas Conference and Exhibition*. Perth: Society of Petroleum Engineers.

26. Ning, J., Liu, X., Tan, Y., Wang, J., & Tian, C. (2015). Relationship of box counting of fractured rock mass with Hoek-Brown 396 parameters using particle flow simulation. Geomechanics and Engineering, 9(5), 619-629.

27. Nguyen NHT, Bui HH, Nguyen GD, Kodikara J. A cohesive damage-plasticity model for DEM and its application for numerical investigation of soft rock fracture properties. International Journal of Plasticity. 2017;98:175-96.

28. Nguyen NHT, Bui HH, Nguyen GD, Kodikara J, Arooran S, Jitsangiam P. A thermodynamics-based cohesive model for discrete element modelling of fracture in cemented materials. International Journal of Solids and Structures. 2017;117:159-76.

29. Papamichos E, Liolios, P., and van den Hoek, P.J. (2004). Breakout stability experiments and analysis. In: 6th North America Rock Mechanics Symposium. Houston: American Rock Mechanics Association.

30. Papamichos E, Tronvoll J, Skjaerstein A, Unander TE (2010) Hole stability of red wildmoor sandstone under anisotropic stresses and sand production criterion. J Pet Sci Eng 72:78–92

31. Potyondy, D. O. (2015) “The bonded-particla model as a tool for rock mechanics research and application: current trends and future directions” Geosyst. Eng., 18(1), 1-28

32. Saidi, F., Bernabe, Y. & Reuschle, T. (2003). The mechanical behavior of synthetic, poorly consolidated granular rock under uniaxial compression. *Tectonophysics*, 370, pp.105-120.

33. Schöpfer, M. P., Childs, C., & Walsh, J. J. (2007). Two-dimensional distinct element modeling of the structure and growth of 381 normal faults in multilayer sequences: 1. Model calibration, boundary conditions, and selected results. Journal of Geophysical 382 Research: Solid Earth, 112(B10).

34. Tian, W. L., & Yang, S. Q. (2017). Experimental and numerical study on the fracture coalescence behavior of rock-like materials 398 containing two non-coplanar filled fissures under uniaxial compression. Geomechanics and Engineering, 12(3), 541-560.

35. Vesga, L. F., Vallejo, L. E., & Lobo-Guerrero, S. (2008). DEM analysis of the crack

propagation in brittle clays under uniaxial 394 compression tests. International journal for numerical and analytical methods in geomechanics, 32(11), 1405-1415.

36. Wu, B., Chen, Z. and Zhang, X. (2016). Stability of Borehole with Breakouts - An Experimental and Numerical Modelling Study. In: 50th US Rock Mechanics/Geomechanics Symposium. Houston: American Rock Mechanics Association

37. Xu, W. J., Li, C. Q., & Zhang, H. Y. (2015). DEM analyses of the mechanical behavior of soil and soil-rock mixture via the 3D 400 direct shear test. Geomechanics & engineering, 9(6), 815-827.

38. Yang B, Jiao Y, Lei S (2006) A study on the effects of microparameters on macroproperties for specimens created by bonded particles. Eng Comput 23:607–631.

39. Zhao W, Huang R, Yan M (2015) Mechanical and fracture behavior of rock mass with parallel concentrated joints with different dip angle and number based on PFC simulation. Geomech Eng 8:757–767.

40. Zhou C, Xu C, Karakus M, Shen J (2018) A systematic approach to the calibration of micro-parameters for the flat-jointed bonded particle model. Geomech Eng 16:471–482.

# Chapter 4

# Development and Application of Laboratory-Scale Convergence Measuring Device in Monitoring Borehole Condition

# (Conference Paper 1, Published)

Jun Hyuk Heo, Noune Melkoumian and Sam S. Hashemi

School of Civil, Environmental and Mining Engineering

The University of Adelaide, SA 5005, Australia

Publication:

Heo, J. H., Melkoumian, N. & Hashemi S. S. (2018). Development and Application of Laboratory-Scale Convergence Measuring Device in Monitoring Borehole Condition.

# Statement of Authorship

| | |
|---|---|
| Title of Paper | Development and Application of Laboratory-Scale Convergence Measuring Device in Monitoring Borhole Condition |
| Publication Status | ☑ Published ☐ Accepted for Publication<br>☐ Submitted for Publication ☐ Unpublished and Unsubmitted work written in manuscript style |
| Publication Details | Heo, J.H, Melkoumian, N. & Hashemi S. S. (2018). Development and Application of Laboratory-Scale Convergence Measuring Device in Monitoring Borehole Condition. In 52nd U.S. Rock Mechanics/ Geomechanics Symposium. Seattle, the United States. |

## Principal Author

| | |
|---|---|
| Name of Principal Author (Candidate) | Jun Hyuk Heo |
| Contribution to the Paper | Performed laboratory tests using the Convergence Measuring Device, interpreted results, developed the manuscript and acted as the corresponding author. |
| Overall percentage (%) | 70% |
| Certification: | This paper reports on original research I conducted during the period of my Higher Degree by Research candidature and is not subject to any obligations or contractual agreements with a third party that would constrain its inclusion in this thesis. I am the primary author of this paper. |
| Signature | Date 02/09/2022 |

## Co-Author Contributions

By signing the Statement of Authorship, each author certifies that:

i. the candidate's stated contribution to the publication is accurate (as detailed above);

ii. permission is granted for the candidate in include the publication in the thesis; and

iii. the sum of all co-author contributions is equal to 100% less the candidate's stated contribution.

| | |
|---|---|
| Name of Co-Author | Dr. Noune Melkoumian |
| Contribution to the Paper | Supervised with research conceptualisation, data interpretation, methodology and reviewed the manuscript. |
| Signature | Date 25.09.2022 |

| | |
|---|---|
| Name of Co-Author | Dr. Sam S. Hashemi |
| Contribution to the Paper | Supervised with methodology, data analysis and reviewed the manuscript. |
| Signature | Date 02/09/2022 |

Please cut and paste additional co-author panels here as required.

# Abstract

Considerable stability problems, such as weakening of the rock formation and borehole convergence, can occur when drilling into areas comprising a poorly cemented formation. In this study, a laboratory-scale convergence measuring device (CMD) has been developed based on the local deformation transducer (LDT) concept, and successfully applied in a series of laboratory tests to continuously monitor borehole deformation in synthetic thick-walled hollow cylinder (TWHC) specimens with various cement contents. Displacement measurements obtained from the CMD were calibrated against a digital micrometer. Calibration results showed that the performance of the CMD and the digital micrometer matched with high accuracy. TWHC test results showed that an increase in the cement content resulted in an increase in the deviatoric stress required to initiate a borehole convergence. Moreover, it was observed that the increment in the level of the deviatoric stress required for the borehole convergence initiation decreased, as the confining pressure increased. These findings can help design more appropriate support systems for drilling operations involving exploration boreholes, as well as oil and gas wellbores to improve the drilling performance in poorly cemented formations.



Keywords: Convergence, thick-walled hollow cylinder, borehole convergence, drilling, poorly cemented formation, stability problems


# 1. Introduction

Borehole instability involving convergence can result in the borehole collapse in weak underground formations. The majority of oil and gas reservoirs are located in weak sedimentary formations where particles are not strongly bonded, resulting in weakening of the rock formation in the vicinity of the borehole and often leads to a borehole convergence. This causes the drilling operations to stop in extreme cases. Monitoring the borehole

condition and gaining a better understanding of it is essential for early detection of instability issues and minimizing borehole failure. While various convergence measuring devices such as caliper log, borehole extensometer, and convergence monitor are being used in the field, relatively few efforts have been made to accurately measure the borehole convergence in laboratory experiments for weak rocks. The cell of Bonnechere, the USBM gage and the CSIRO HI cell have been proposed for laboratory-based tests to measure the borehole deformation (Amadei and Stephansson, 1997). However, their application requires an extensive installation procedure and is limited to a specific borehole diameter size matching the size of the monitoring device, i.e. the diameter must be more than 30 mm. In the current study a cost-effective, versatile and reliable convergence measuring device with a quick and easy installation procedure was developed based on the concept of the LDT proposed by Goto et al. (1991) to evaluate the borehole deformation in thick-walled hollow cylinder specimens. These new CMDs have been calibrated and tested in laboratory conditions in order to verify their performance under different stress paths for poorly cemented sands.

Laboratory experiments involving the measurement of the diametric deformation of a borehole by placing a two-arm caliper inside a hollow cylinder were carried out by Tronvoll (1992). However, the effect of different stress paths was not investigated. Igarashi et al. (2008) developed a borehole tangential deformation gage to measure the tangential deformation of the borehole wall. Papamichos et al. (2010) performed laboratory experiments on hollow cylinder specimens of Red Wildmore sandstone where they used cantilever strain gage pairs to study the effect of the stress anisotropy on the borehole deformation. Bujok et al. (2013) conducted experimental studies on the effects of the well convergence on the deformational shape of the borehole. Wu et al. (2016) conducted polyaxial tests with a four-arm cantilever borehole gage placed inside the borehole within a block specimen to measure the borehole

deformation. These tests involved a relatively stronger sandstone with a uniaxial compressive strength (UCS) of greater than 10 MPa.

Borehole stability studies employ TWHC tests to investigate physical mechanisms by pressurizing the outer boundary of the TWHC specimens while monitoring the behaviour of the internal borehole surface (Tronvoll and Fjaer, 1994). In this work, a series of TWHC tests were performed on poorly cemented sandstone specimens, with the UCS of no greater than 10 MPa, under various stress paths and with the CMDs placed inside the borehole to measure convergence. The aim was to investigate the accuracy and performance of the newly developed CMD and the failure behaviour of poorly cemented formations near an opening and under different stress paths.

# 2. Convergence measuring device

The proposed convergence measuring device (CMD) was developed using the concept of the LDT. This concept was originally developed by Goto et al. (1991) with the aim to minimize the error in the measurement of the average local strain associated with the traditional method of attaching strain gages directly on the surface of the specimens. The measurements obtained by Goto et al. (1991) presented a high level of accuracy for both monotonic and cyclic loading test conditions.

The design of the CMD is given in Fig. 1. It consists of two metal legs with a strain gage attached to both outer surfaces of the metal frame to measure strain changes. PVC plastic beads are attached to the outer surfaces of the CMD leg tips to minimize the friction between the CMD and the borehole wall. As the distance (*d*) between the two legs of the CMD (see Fig.1 (b)) changes with the change in the borehole diameter and causes deflection of the CMD legs, subsequently this deflection is detected by the strain gages on the metal frame. To

convert the measured strain unit (S) to a displacement unit (mm) the laboratory software NIMEX was used. Fig.1 (c) shows the actual CMD manufactured for testing.

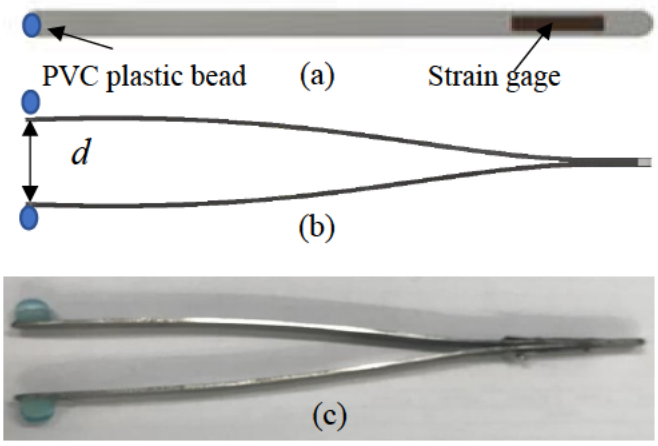


Fig. 1. Convergence measuring device (a) Side view of the CMD, (b) Top view of the CMD, (c) Actual CMD prepared for testing

Calibration of the CMD was carried out to verify the displacement outputs. For this Mitutoyo Digimatic Micrometer 164 was used. Fig. 2 shows the calibration setup, where the CMD was placed against the digital micrometer. The CMD was contracted from the original position to set the distance between the CMD legs at 15 mm to match it with the size of the borehole of the TWHC specimens to be tested. As the strain changes detected by the strain gages from the deflections of the CMD legs are proportional to the change in the distance -*d*- between the legs, the initial displacement output from the CMD was zeroed and the subsequent outputs were used for calibration. The calibration process involved comparing the digital micrometer and the CMD outputs, and adjusting the CMD reading accordingly to match it with the reading from the digital micrometer. Measurements were taken at 0.1 mm intervals to analyze and adjust the discrepancy between the CMD and the calibrator, and to achieve a high level of accuracy.

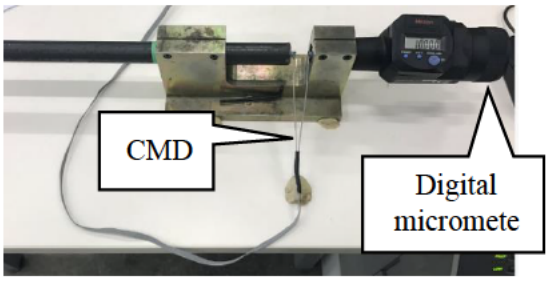


Fig. 2. Calibration of the CMD

Fig. 3 presents the calibration result. Displacement readings from the CMD and the calibrator were plotted versus the time to assess the accuracy of the CMD. The displacement output from the CMD accurately matched with the displacement output from the digital micrometer with a negligible error only.

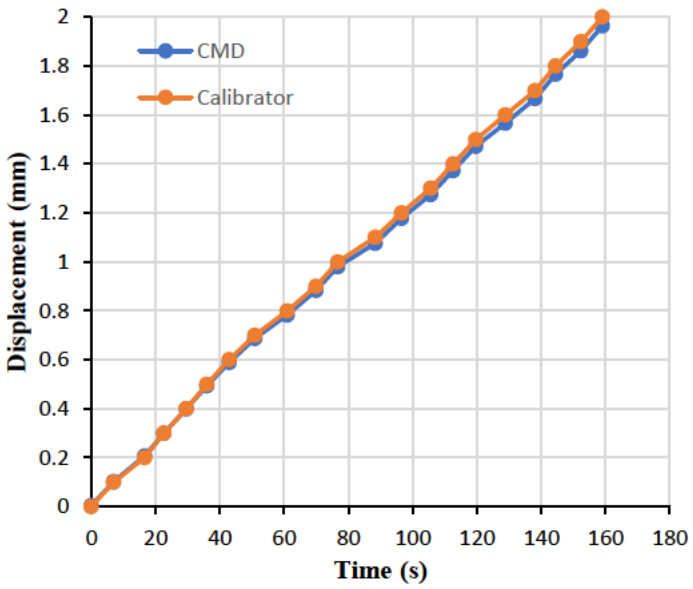


Fig. 3. Calibration result for the CMD

# 3. Experimental methods

*3.1 Specimen preparation*

Synthetic poorly cemented sandstone specimens were prepared by mixing Portland cement type II (specific gravity, $Gs$ = 3.15 $g/cm^3$), sand grains and water. The specimen preparation procedure proposed by Hashemi and Melkoumian (2016) was followed. For specimen

preparation, two different sand grain sizes, namely coarse grain with a diameter range of 0.425 mm-1.4 mm and fine grain with a diameter range of 0.15 mm-0.355 mm were mixed at a 50:50 ratio. Various cement contents ranging between 10% ~ 14% were used to ensure that the prepared specimens had a UCS of less than 10 MPa, and could replicate the characteristics of a poorly cemented sandstone. Preliminary studies showed that the cement content above 14% yields an undesirable high strength, and 14% of cement content was set as the upper limit for the specimen preparation.

Fig. 4 shows cylindrical weak sandstone specimens after UCS testing. An MTS C45 testing machine was used for UCS tests, and the specimen was prepared to be 36.5 mm in diameter and 127 mm in height. For each cement content (CC), three tests were carried out.

Fig. 4. Specimens after the failure in UCS tests

The average porosity of the tested specimens was 18±3 % and the average UCS ranged from 4.98 MPa to 9.78 MPa as is shown in Table 1. The calculated bulk density for each CC is also shown in the table.

Table 1. Mechanical properties of the TWHC specimens

| | 10% CC | 12% CC | 14% CC |
|---|---|---|---|
| UCS (MPa) | 4.98 | 7.69 | 9.78 |
| Porosity (%) | 18±3 | 18±3 | 18±3 |
| Bulk density $p$(kg/m$^3$) | 1792 | 1859 | 1913 |

*3.2 Experimental setup*

All tests were performed on TWHC specimens with a height of 128 mm, and with a 36.5 mm outer diameter and 15 mm inner diameter. The TWHC specimen was placed inside the Hoek cell with two CMDs placed inside the borehole as is shown in Fig. 5. To monitor the borehole deformation both CMDs were positioned approximately 42 mm from the borehole opening, i.e. where the largest deformation is expected to occur based on the preliminary tests. A micro camera was positioned on top of the TWHC specimen to visually monitor the borehole deformation process. The external stresses were generated by applying a confining pressure at the outer boundary of the specimen using the Hoek cell.

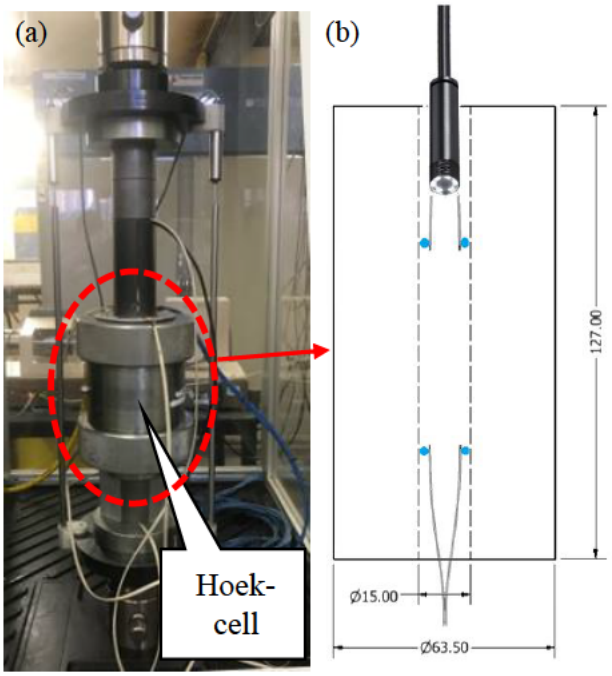


Fig. 5. Experimental apparatus (a) the test setup, (b) the schematic diagram of the thick-walled hollow cylinder placed inside the Hoek cell

The inside view of the TWHC specimen from the camera is presented in Fig. 6. As the CMDs were positioned inside the borehole, the TWHC tests allowed to examine their capability in measuring the borehole deformation under various stress conditions.

Fig. 6. Inside view of the TWHC specimen from the micro camera

TWHC tests were performed under various stress paths as is shown in Eq. (1a-c). In the first stress path (Eq. 1a), hydrostatic stress condition was applied in the first step followed by increasing the axial stress ($\sigma_z$) at a rate of 0.07 mm/s until the borehole breakout was observed

by the camera. In the second stress path, hydrostatic stress condition was applied in the first step, followed by increasing the confining pressure ($\sigma_{conf}$) at a rate of 0.2 MPa/min until the borehole breakout was observed. In the third stress path (Eq. 1c), both $\sigma_\theta$ and $\sigma_r$ were increased simultaneously at the same rate until the failure at the borehole wall was observed by the camera.

$$1^{st}\ \text{path stress} \begin{cases} \sigma_1 = \sigma_2 = \sigma_3 = \sigma_{conf} = \sigma_z (\text{first step}) \\ \sigma_1 = \sigma_z > \sigma_2 = \sigma_3 = \sigma_{conf} (\text{second step}) \end{cases} \quad (1a)$$

$$2^{nd}\ \text{stress path} \begin{cases} \sigma_1 = \sigma_2 = \sigma_3 = \sigma_{conf} = \sigma_z (\text{first step}) \\ \sigma_1 = \sigma_2 = \sigma_{conf} > \sigma_3 = \sigma_z (\text{second step}) \end{cases} \quad (1b)$$

$$3^{rd}\ \text{stress path} \begin{cases} \sigma_1 = \sigma_\theta = \sigma_1 = \sigma_z > \sigma_r = 0 (\text{first step}) \\ \sigma_1 = \sigma_\theta = \sigma_1 = \sigma_z > \sigma_r = 0 (\text{second step}) \end{cases} \quad (1c)$$

Various deformation shapes were observed from the tests as is shown in Fig. 7. The first stress path resulted in the slot like failures as can be seen in Fig. 7 (a). This type of failure was also observed by Papamichos et al. (2010) from testing weak hollow cylinder sandstone specimens under isotropic stresses. The deformation from the second stress path where a constant increase in the confining stress was applied onto the outer boundary of the specimen shows that the borehole wall has collapsed, and loose sand particles have filled the borehole as can be seen in Fig. 7 (b). Similar failure was observed for the third stress path as seen in Fig. 7 (c).

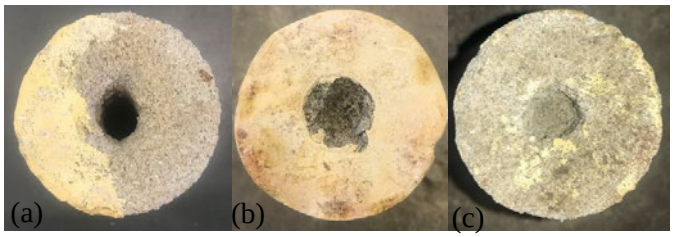


Fig. 7. TWHC specimens with various deformation shapes, (a) Specimen tested under the stress path 1 (Eq.1a), (b) Specimen tested under the stress path 2 (Eq. 1b), (c) Specimen tested under the stress path 3 (Eq.1c)

# 4. Results and discussions

Laboratory tests were conducted on TWHC specimens with the CMDs placed inside the borehole to investigate the failure behaviour of the poorly cemented sandstone under various stress paths. A video camera was employed to monitor the borehole deformation process. Test

results showed that the increase in the cement content resulted in a considerable increase in the deviatoric stress ($\sigma_{deviatoric} = \sigma_1 - \sigma_{hydrostatic}$) required to initiate the borehole convergence. Moreover, it was observed that the increment in the level of the deviatoric stress required for the borehole convergence initiation decreased, as the confining pressure increased.

*4.1 Thick-walled hollow cylinder tests*

Fig. 8 presents the deviatoric stress ($\sigma_1 - \sigma_3$) versus the radial strain ($\varepsilon_r$) response of the TWHC specimens tested under the first stress path (Eq. 1a). The specimens with 10% cement content were tested at various hydrostatic stress conditions (i.e. 2 MPa, 4 MPa and 6 MPa). The increase in the initial hydrostatic stress from 2 MPa to 4 MPa resulted in an increase from 3.95 MPa to 4.69 MPa in the deviatoric stress required to initiate a borehole convergence (yield stress), and a further increase in the hydrostatic stress to 6 MPa resulted in the decrease in the deviatoric stress to 3.41 MPa. This is likely to be due to the higher confining pressure and vertical stress applied to the specimen during the first step resulting in an earlier initiation of the borehole convergence as the specimen failed due to the high stresses applied during the second step.

The increase from 10% to 12% in the cement content for specimens tested under 6 MPa of hydrostatic stress condition resulted in a slight increase from 3.41 MPa to 4.46 MPa in the yield deviatoric stress. However, the deviatoric stress required to initiate a borehole convergence was 2.54 times higher (i.e. 11.34 MPa) in the specimen with the cement content of 14% than it was in the specimen with 12% cement content. This behavior in the TWHC specimens with a higher cement content of 14% is associated with the strengthening effect of the cement.

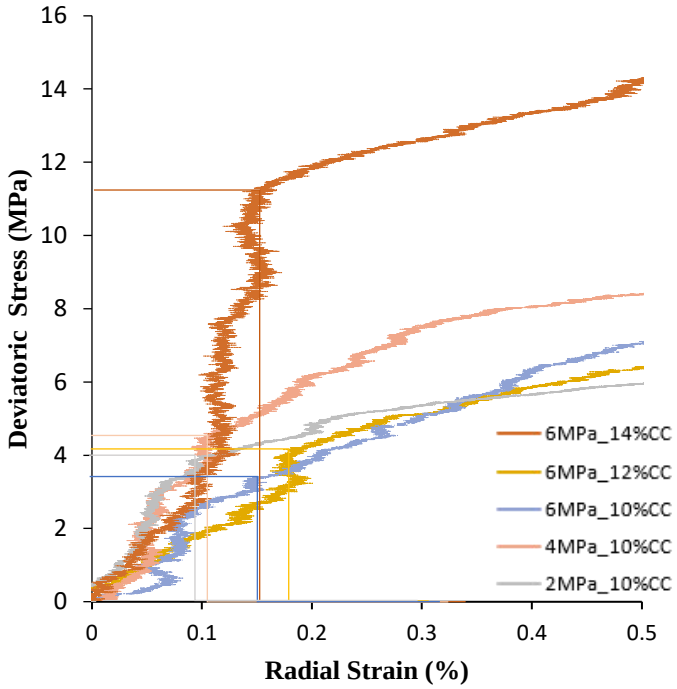


Fig. 8. Thick-walled hollow cylinder test results for the first stress path

The TWHC specimens with different cement contents ranging from 10% ~ 14% were tested under the second stress path (Eq. 1b). The increase in the cement content had a minimal influence on the stiffness of the specimens as can be seen in Fig 9. Mogi (2007) suggested that the stiffness depends on the rock material and, as the same sand grain sizes were used for the specimen preparation, the specimen stiffness remained unchanged in the tests. The level of the confining pressure required to initiate a borehole convergence increased with the increase in the cement content. This is due to the strengthening effect of the cement. Hashemi et al. (2015) have also observed that the poorly cemented specimens with a higher cement content demonstrate a higher peak strength due to the strengthening effect of the cementing agent. Fig. 9a-b illustrate the borehole failure process as observed from the camera installed inside the borehole.

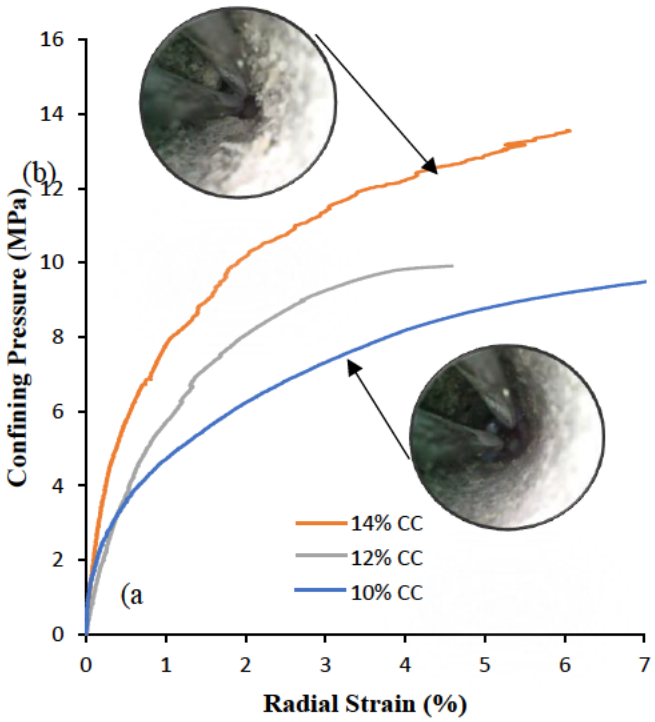


Fig. 9. Thick-walled hollow cylinder test results for the second stress path, (a) Initiation of the borehole convergence captured by the camera, (b) Borehole failure observed from the camera

The TWHC test results from the third stress path (Eq. 1c) are shown in Fig. 10. While the yield stresses increase consistently with the increase in the cement content, the specimens with 12% cement content behaved differently. For these specimens, the measured radial strain was significantly higher at a lower stress state of 2.77 MPa, compared to the specimens with 10% and 14% of cement content. This is likely to be caused by one of the two CMDs being placed at a location in the borehole where the borehole converged significantly more than at the other CMD. Therefore, the averaging of the two CMD readings resulted in such a different reading compared to the results obtained for the other cement contents. The yield stress for the 10% cement content was 11.18 MPa, whereas it was 24.20 MPa for the 14% cement content. The TWHC specimens with 10% and 14% cement content behaved similarly as is indicated by the stress versus radial strain behavior.

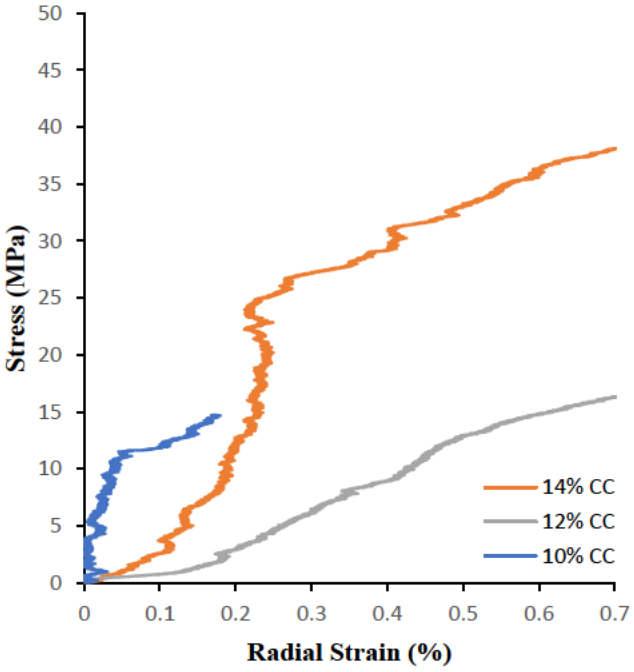


Fig. 10. Thick-walled hollow cylinder test results for the third stress path

# 5. Conclusions

The proposed convergence measuring device (CMD) was designed and manufactured to be used for accurately measuring the borehole deformation in laboratory-based studies. In this study, it was used to measure the borehole convergence in poorly cemented TWHC specimens under various testing conditions. For this, the CMD was installed inside the 15 mm diameter borehole of the TWHC specimens. The CMD was calibrated against the digital micrometer, and the performance of the CMD under different stress paths was examined. The calibration result showed that the CMD provides accurate readings. Also, it has been demonstrated that the CMDs can be successfully used for continuously measuring borehole deformation during the TWHC tests by installing them inside the borehole of a TWHC specimen. The TWHC test results showed that the increase in the cement content from 12% to 14% resulted in 2.54 times higher deviatoric stress required to initiate a borehole convergence under the first stress path. Moreover, it was observed that the increment in the

level of the deviatoric stress required for the borehole convergence initiation decreased, as the hydrostatic stress condition was increased from 4 MPa to 6 MPa. The specimens tested under the second and the third stress path showed the significance of the strengthening effect of the cementing agent.

# 6. References


1. Amadei, B. and O. Stephansson. 1997. Rock stress and its measurement. 1st ed. Chapman & Hall
2. Bujok, P., M. Prozer, K. Labus, M. Klempa, J. Pavlus. 2013. Experimental modelling of abandoned shallow oil wells convergence. Engineering Geology, 157, pp.1-7.
3. Goto, S. F. Tatsuoka, S. Shibuya, Y.S. Kim, T. Sato. 1991. A simple gauge for local small strain measurements in the laboratory. Soils and Foundations. Vol. 31 No. 1, 169-180.
4. Hashmi, S.S., N. Melkoumian, A. Taheri and M. Jaksa. 2015. The failure behavior of poorly cemented sands at a borehole wall using laboratory tests. International journal of Rock Mechanics and Mining Science. 77:pp.348-357.
5. Hashmi, S.S. and N. Melkoumian. 2016. Effect of different stress path regimes on borehole instability in poorly cemented granular formations. Journal of Petroleum Science and Engineering. 146:pp.30-49.
6. Igarashi. A., T. Ito, K. Sekine and K. Hayashi. 2008. Development of borehole tangential deformation gage and its application for determining the stress in rock. In Proceedings of the 42nd US Rock Mechanics Symposium and 2nd U.S. - Canada Rock Mechanics Symposium, San Francisco, 29 June – 2 July 2008.
7. Mogi, K. Experimental rock mechanics. London: Taylor and Francis; 2007

8. Papamichos, E., J. Tronvoll, A. Skjaerstein and T.E. Unander. 2010. Hole stability of Red Wildmoor sandstone under anisotropic stresses and sand production criterion. J. Petroleum Science and Engineering. Res. 72:78-92
9. Tronvoll, J. Experimental Investigation of Perforation Cavity Stability. 1992. In Proceedings of the 33rd U.S. Symposium on Rock Mechanics, Santa Fe, 3 - 5 June 1992, eds. J.R. Tillerson & W.R. Wawersik, 365-373. Rotterdam: Balkema.
10. Tronvoll, J., and E. Fjaer. 1994. Experimental studies of sand production from perforation cavities. Int. J. Rock Mech. & Min. Sci., 31(5): 393–410
11. Wu, B., Z. Chen and X. Zhang. Stability of borehole with Breakouts – An Experimental and Numerical Modelling Study. ARMA 16-466 presented at the 50th US Rock Mechanics/Geomechanics Symposium, Houston, Texas. USA.

# Chapter 5

## 1. Concluding Remarks

Thesis provides comprehensive study on the failure behaviour of poorly cemented sandy formations, namely sandstone.

A new modified laboratory test method and laboratory scale Convergence Measuring Device have been designed and implemented for real-time monitoring of the borehole status during the triaxial tests.

The effects of five different stress path regimes and three different cement contents on the borehole failure have been investigated using TWHC tests. In the first and second stress path, the vertical stress and the confining pressure were considered. In the third, fourth and fifth stress path, the principal stresses were considered. The results showed that the increase in the cement content increased the radial strain under the first stress path. The increase in the cement content had a minimal effect on the stiffness of the specimens under the second stress path. The specimens under the third stress path showed that the radial strain increased with the increase in the cement content. The effect of the cement content had a lesser influence on the borehole failure under the fourth stress path than the change in the vertical stress had. The specimens under the fifth stress path tolerated a higher level of stresses. The effect of the cement content on the borehole failure was found to be more significant than the effect of the confining pressure under all stress paths.

Numerical simulations of the borehole failure using Discrete Element Method (DEM) have been performed to evaluate and assess the influence of micro-parameters such as stiffness ratio, friction angle, friction coefficient and effective modulus on the borehole failure. For this the software PFC2D was used, and the results from numerical simulations were verified by comparing them with the results obtained from the laboratory studies. A series of numerical

simulations were conducted to achieve the calibrated numerical model that could successfully simulate the behaviour of poorly cemented sandstone specimens tested in laboratory. The numerical simulation results showed a good agreement with the stress-displacement data from their experimental counterparts.

Further research on the following topics is recommended to gain a better understanding on the borehole stability in poorly cemented sandy formations, namely in sandstones: (1) consider other cement contents, (2) conduct true-triaxial tests to study the three-dimensional stress-strain-strength behaviour, (3) conduct true-triaxial simulation using the discrete element method.